Received: 1 August 2016 | Revised: 24 February 2017 | Accepted: 31 March 2017

DOI: 10.1002/hipo.22732

RESEARCH ARTICLE

WILEY

# Effects of M1 and M4 activation on excitatory synaptic transmission in CA1

Catherine A. Thorn | Michael Popiolek | Eda Stark | Jeremy R. Edgerton

Pfizer Internal Medicine Research Unit, Cambridge, Massachusetts 02139

**Correspondence**
Jeremy R. Edgerton, 1 Portland St., 406.2, Cambridge, MA 02139, USA.
Email: jeremy.edgerton@pfizer.com

## Abstract

Hippocampal networks are particularly susceptible to dysfunction in many neurodegenerative diseases and neuropsychiatric disorders including Alzheimer's disease, Lewy body dementia, and schizophrenia. CA1, a major output region of the hippocampus, receives glutamatergic input from both hippocampal CA3 and entorhinal cortex, via the Schaffer collateral (SC) and temporoammonic (TA) pathways, respectively. SC and TA inputs to CA1 are thought to be differentially involved in the retrieval of previously stored memories versus the encoding of novel information, and switching between these two crucial hippocampal functions is thought to critically depend on acetylcholine (ACh) acting at muscarinic receptors. In this study, we aimed to determine the roles of specific subtypes of muscarinic receptors in mediating the neuromodulatory effects of ACh on glutamatergic synaptic transmission in the SC and TA pathways of CA1. Using selective pharmacological activation of M1 or M4 receptors along with extracellular and intracellular electrophysiology recordings from adult rat hippocampal slices, we demonstrate that activation of M1 receptors increases spontaneous spike rates of neuronal ensembles in CA1 and increases the intrinsic excitability of pyramidal neurons and interneurons. Selective activation of M4 receptors inhibits glutamate release in the SC pathway, while leaving synaptic transmission in the TA pathway comparatively intact. These results suggest specific mechanisms by which M1 and M4 activation may normalize CA1 circuit activity following disruptions of signaling that accompany neurodegenerative dementias or neuropsychiatric disorders. These findings are of particular interest in light of clinical findings that xanomeline, an M1/M4 preferring agonist, was able to improve cognitive and behavioral symptoms in patients with Alzheimer's disease or schizophrenia.

**KEYWORDS**

acetylcholine, electrophysiology, muscarinic, Schaffer collateral, temporoammonic

## 1 | INTRODUCTION

Pyramidal neurons in the CA1 region of the hippocampus integrate glutamatergic inputs from two distinct sources that play complementary roles in the memory retrieval and encoding functions for which the hippocampus is well known. Schaffer collateral (SC) inputs carry information retrieved from the dentate-CA3 networks supporting pattern separation and completion (Kesner, Kirk, Yu, Polansky, & Musso, 2016; Knierim & Neunuebel, 2016; O'Reilly & McClelland, 1994; Myers & Scharfman, 2011; Rolls & Kesner, 2006), whereas temporoammonic (TA) inputs from the entorhinal cortex convey information related to the animal's current environment for encoding (Cutsuridis, Cobb, & Graham, 2010; Hasselmo & Schnell, 1994; Hasselmo, Schnell, & Barkai, 1995; Hasselmo & Wyble, 1997; Knierim & Neunuebel, 2016). A long-standing question is how the same hippocampal circuitry can support memory retrieval and memory encoding processes without corruption of either pre-existing or new information.

Cholinergic state switching is one proposed mechanism by which these important functions may be spatially and temporally separated within the hippocampal network (Hasselmo & Bower, 1992; Hasselmo

& Schnell, 1994), and a large body of research has revealed several specific actions of ACh within the hippocampus that are thought to underlie the modulation of memory encoding versus retrieval processes. High levels of ACh have been shown to suppress SC synaptic transmission (Dasari & Gulledge, 2011; Hounsgaard, 1978; Hasselmo & Schnell, 1994; Valentino & Dingledine, 1981) and enhance several forms of synaptic plasticity (Drever, Riedel, & Platt, 2011; Teles-Grilo Ruivo & Mellor, 2013), whereas low cholinergic tone has been shown to reactivate the autoassociative dentate-CA3 network during memory consolidation (Buzsaki, 1989; Deiana, Platt, & Riedel, 2011; Gais & Born, 2004; Hasselmo et al., 1995; Hasselmo, 1999). Furthermore, ACh has been shown to differentially regulate SC and TA synapses (Hasselmo & Schnell, 1994), strongly suppressing SC inputs to CA1 while sparing TA inputs. Differential expression of presynaptic muscarinic receptors (mAChRs) within the two pathways is one factor suggested to underlie these effects (Cea-del Rio et al., 2010; Dasari & Gulledge, 2011; Easton, Douchamps, Eacott, & Lever, 2012; Fernandez de Sevilla & Buno, 2003; Hasselmo & Schnell, 1994; Leung & Peloquin, 2010; Levey, Edmunds, Koliatsos, Wiley, & Heilman, 1995; Qian & Saggau, 1997; Shirey et al., 2008).

While it is clear that mAChRs modulate the learning and memory functions of the hippocampus (Deiana et al., 2011; Thiele, 2013; Wilson & Fadel, 2016), the contributions of specific mAChR subtypes in mediating these effects remain unclear. Early immunohistochemical (Hersch & Levey, 1995; Levey et al., 1995) and *in situ* hybridization (Brann, Buckley, & Bonner, 1988; Buckley et al., 1988) studies showed predominant M1, M2, and M4 mAChR protein and gene expression within the hippocampus, with $G_{i/o}$-coupled M2 and M4 receptors largely located presynaptically (Levey et al., 1995; Rouse, Edmunds, Yi, Gilmor, & Levey, 2000), and $G_{q/11}$-coupled M1 receptors largely located postsynaptically (Levey et al., 1995; Rouse et al., 2000; Volpicelli & Levey, 2004). Across the five mAChR subtypes, the orthosteric ACh binding pocket is highly conserved (Kruse et al., 2014; Lu, Saldanha, & Hulme, 2002; ), making it very difficult to develop subtype-selective activators and inhibitors. As a result, functional studies have largely relied either on transgenic knockout animals susceptible to compensatory receptor expression or on nonselective pharmacological manipulations to identify the mechanisms underlying the actions of ACh on the different mAChR subtypes within the hippocampus. These studies point to the involvement of presynaptically expressed M4 receptors in ACh-mediated SC suppression (Dasari & Gulledge, 2011; Sanchez et al., 2009; Shirey et al., 2008), though M1 (Kremin et al., 2006; Leung & Peloquin, 2010; Sheridan & Sutor, 1990), M2 (Seeger & Alzheimer, 2001), and M3 (de Vin, Choi, Bolognesi, & Lefebvre, 2015) receptors have also been implicated in this effect. Activation of postsynaptic M1 receptors has been linked to long-term potentiation at SC synapses (Boddeke, Enz, & Shapiro, 1992; Buchanan, Petrovic, Chamberlain, Marrion, & Mellor, 2010; Dasari & Gulledge, 2011; Giessel & Sabatini, 2010), and to excitation of CA1 pyramidal cells (Dasari & Gulledge, 2011) and interneurons (Bell, Bell, & McQuiston, 2015a; Yi et al., 2014).

In light of clinical evidence suggesting that xanomeline, an M1/M4 preferring agonist, improves cognitive and behavioral symptoms in patients with Alzheimer's disease (Bodick et al., 1997) or schizophrenia (Shekhar et al., 2008), it is of interest to clarify the effects of selective pharmacological activation of M1 or M4 receptors on CA1 circuit function. Recently, significant progress has been made in developing selective agonists and positive allosteric modulators (PAMs) that target these specific subtypes of mAChRs (Chan et al., 2008; Davie, Christopoulos, & Scammells, 2013; Foster, Choi, Conn, & Rook, 2014; Ghoshal et al., 2016; Wess, 2005), but these new tools have not yet been used to dissect the contributions of mAChR subtypes to hippocampal circuit activity. In this study, we took advantage of three recently developed, highly selective M4 activators and one highly selective M1 agonist. These include two M4 PAMs derived from the previously published VU series (Brady et al., 2008; Lindsley et al., 2013), an M4 bitopic agonist (Livermore, White, Congreve, Brown, & O'brien, 2014), and the recently published M1 allosteric agonist GSK1034702 that was tested in a phase I clinical trial (Budzik et al., 2010; Ridley, Pugh, Maclean, & Baker, 1999; Nathan et al., 2013). We performed extracellular field recordings and whole-cell patch clamp recordings in combination with bath application of these selective compounds to demonstrate differential effects of M1 and M4 activation at SC and TA synapses. Activation of M1 receptors enhanced the intrinsic excitability and spontaneous firing rates of CA1 pyramidal cells and interneurons, whereas activation of M4 receptors strongly suppressed synaptic transmission in the SC, but not TA, pathway. These findings support the role of M1 and M4 receptors as prominent drivers of ACh-mediated modulation of CA1 circuits, each independently contributing to the biasing of CA1 toward a network state that could facilitate memory encoding.

## 2 | MATERIALS AND METHODS

Animals were handled and cared for according to the National Institutes for Health Guide for the Care and Use of Laboratory Animals, and all procedures were performed with the approval of the Pfizer Institutional Animal Care and Use Committee.

### 2.1 | Slice preparation

For whole-cell recording experiments and extracellular spike rate recordings, adult (8–12 weeks) male Sprague Dawley rats were deeply anesthetized with isofluorane and perfused transcardially with ice-cold high-sucrose artificial cerebrospinal (ACSF) cutting solution containing 206 mM sucrose, 26 mM $NaHCO_3$, 3 mM KCl, 1.25 mM $NaH_2PO_4$, 7 mM $MgCl_2$, 0.5 mM $CaCl_2$, 10 mM glucose, 1 mM sodium pyruvate, and 0.89 mM sodium L-ascorbate, bubbled with 95% $O_2$/5% $CO_2$. Brains were removed into ice-cold cutting ACSF and coronal hippocampal slices were made (300 μM) using a vibrating microtome. Slices were incubated at 35°C in recording ACSF (124 mM NaCl, 3 mM KCl, 1.25 mM $NaH_2PO_4$, 26 mM $NaHCO_3$, 10 mM glucose, 1.3 mM $MgCl_2$, 2 mM $CaCl_2$, 1 mM sodium pyruvate, and 0.89 mM sodium L-ascorbate) bubbled with 95% $O_2$/5% $CO_2$ for 1–4 hr prior to recording. For extracellular recordings with SC stimulation, rats were deeply anesthetized with isofluorane and rapidly decapitated. All other slice preparation procedures were identical.

## 2.2 | Whole-cell recordings

Intracellular recordings were performed at 35°C in recirculating recording ACSF bubbled with 95% $O_2$/5% $CO_2$. Cells in the CA1 pyramidal cell layer were visualized using a Zeiss LSM 7MP microscope outfitted with a DIR filter, projected to a television screen via a CCD camera and image enhancing controller box (Hamamatsu, Japan). Recording pipettes were filled with internal solution containing (in mM) 130 K-gluconate, 10 HEPES, 5 glutathione, 0.2 EGTA, 4 MgATP·2$H_2O$, 0.4 $Na_3$ GTP·2$H_2O$, 7 $Na_2$-phosphocreatine, 0.05 spermine, and 5 μM Alexa-594 (Molecular Probes) for imaging and morphological confirmation of cell type. Synaptic currents were measured in voltage clamp and stimulating current pulses (30–200 μA) were delivered through bipolar electrodes (FHC, Bowdoin ME) placed in stratum radiatum (SC stimulation) or stratum laculosum moleculare (TA stimulation). All compounds were bath applied and washed on for 10 min before recording. Evoked synaptic transmission experiments were made up of 5 trials consisting of one single-pulse followed by three paired-pulse stimuli with 20, 60, and 100 ms interpulse intervals. Stimulation of SC and TA pathways was interleaved with a 5 s interstimulus interval. Experiments were run using custom PClamp (Molecular Devices, Sunnyvale CA) scripts, which controlled analog and digital output channels of a daq card (National Instruments, Austin TX) that interfaced with a MultiClamp 700B (Molecular Devices, Sunnyvale CA) controlling current and voltage through the whole cell recording pipette and two digital stimulus isolation amplifiers (Getting Instruments, San Diego CA) controlling the delivery of SC and TA bipolar stimulation. Cells with low and accommodating firing rates (< 50 Hz) in response to a +200 pA, 500 ms current injection, and clear sag currents (> 4% of steady-state voltage) were classified as putative pyramidal neurons. Morphology was confirmed following most pyramidal cell recordings using 2-photon imaging of the Alexa-594 filled cells (excitation wavelength = 810 nm, power = 5%, gain = 900). Cells with small sag currents (< 4% of steady-state voltage), narrow spike widths (< 650 μs), and high firing rates (> 50 Hz in response to a 300 pA current step) were classified as putative PV-positive (PV+) interneurons, and in all cases, nonpyramidal morphology was confirmed with fluorescence imaging. Table 1 lists the basic electrophysiological properties for the cells included in each data set; current step responses were not recorded for all pyramidal cells.

## 2.3 | Extracellular recordings

Slices were placed onto MED-P515A 64-channel multielectrode arrays (Alpha MED Scientific Inc., Osaka JP) with the CA1 pyramidal cell layer positioned directly over the array contacts. Recordings were made at 30°C in recirculating recording ACSF bubbled with 95% $O_2$/5% $CO_2$. Spiking activity or evoked potentials were captured using MED64 hardware and Mobius software (MED64 system, Alpha MED Scientific Inc., Osaka JP). Synaptic field potentials were evoked by stimulation of the SC pathway at a contact located in stratum radiatum. Stimulus intensity was determined prior to the start of the experiment as the intensity that produced an evoked field response amplitude 60–80% of the maximum response (10–130 μA, 0.2 ms).

## 2.4 | Test compounds

The M1 agonist GSK1034702 (Nathan et al., 2013; Ridler et al., 2014) and M4 activators PT-1148 (5-amino-3,4-dimethyl-N-(1-(pyridin-3-yl) azetidin-3-yl)thieno[2,3-c]pyridazine-6-carboxamide; Lindsley et al. (2013)), PT-3763 (3-amino-4,6-dimethyl-N-(1-(pyridin-3-yl)azetidin-3-yl)thieno[2,3-b]pyridine-2-carboxamide; Brady et al. (2008); Lindsley et al. (2013)), and PT-6950 (ethyl 4-(4-(2-methoxypyridin-3-yl)piperidin-1-yl)azepane-1-carboxylate; Livermore et al. (2014)) were prepared based on published methods by Pfizer World Wide Medicinal Chemistry. Other chemicals were obtained from Tocris (oxotremorine, picrotoxin, VU0255035), Acros Organics (picrotoxin), and Fisher (DMSO). Concentrated stock solutions (10 mM) were made by dissolving test compounds in either $H_2O$ (pirenzipine) or DMSO (all other compounds) and stored at 4°C for up to 4 weeks. During experiments, small volumes of stock solutions were diluted in the circulating recording ASCF to the desired concentrations. For whole-cell experiments, picrotoxin was dissolved directly in recording ASCF made fresh on the day of recording.

## 2.5 | Data analysis

For extracellular MED64 recordings, evoked synaptic field potentials (fSPs) or spontaneous spike rates were recorded from 16 channels spanning stratum pyramidale and striatum radiatum of CA1. Data were captured using MED64 hardware and Mobius software (MED64 system, Alpha MED Scientific Inc.) and analyzed using custom Matlab scripts (MathWorks Inc., Natick MA).

During fSP recording experiments, escalating concentrations of compounds were bath applied to each slice and each concentration was applied for at least 20 min. Dose-response curves for fSP responses were constructed by first computing the amplitude of each evoked fSP as the minimum voltage reached within 25 ms following stimulus onset. The mean fSP amplitude for each channel was then computed for the last 15 trials in the time window corresponding to administration of each concentration of compound and normalized to the mean fSP amplitude during an initial drug-free baseline period. Mean normalized fSP amplitude for each concentration was computed for each slice by averaging across all channels on which baseline fSPs with amplitudes > 200 μV were recorded. Statistical analysis was performed in R (R Core Team, 2016) using the "drc" package (Ritz, Baty, Streibig, & Gerhard, 2015). Mean data from each slice were used to find the best fit to a four-parameter logarithmic function of the form $DR(x) = C + (D - C)/(1 + \exp(B \times (\ln(x) - \ln(E))))$, for drug concentrations $x$. Lower asymptote values (parameter $C$) were compared using pairwise $t$-tests and $p$ values were corrected for multiple comparisons using false discovery rate method. A significant difference is reported for corrected $p$ values $< 0.05$.

For spontaneous spike recordings, data were captured in 30 s epochs every 1.5 min. For each epoch, data were bandpass filtered (600–9000 Hz), and spikes were identified at time points when the voltage exceeded 5 standard deviations from the mean voltage for the entire epoch. For each channel, the mean number of spikes per epoch occurring during the administration of each concentration of compound was calculated, and $z$-score normalized using the mean and standard deviation of the number of spikes per epoch occurring during the initial baseline period. For each slice, a mean $z$-score normalized

**TABLE 1** Electrophysiological characteristics of the pyramidal cells included in the M4 PAM whole cell experiments shown in Figure 3 (PT-4811 and PT-3763), pyramidal cells included in the GSK1034702 experiments shown in Figure 5, and interneurons included in the GSK1034702 experiments shown in Figure 5g

| | $V_m$ (mV) | $R_{IN}$ (MΩ) | Sag @ −200 pA Minimum (mV)/ steady state (mV) | Sag @ −200 pA % ss voltage (peak − ss)/ss | Firing rate @ +200 pA (Hz) | Spike frequency adaptation (ISI5/ISI1) |
|---|---|---|---|---|---|---|
| PT-4811 | −60.0 | 161.0 | | | | |
| | −63.3 | 153.3 | | | | |
| | −62.6 | 100.4 | | | | |
| | −56.6 | 112.4 | | | | |
| | −60.5 | 154.1 | | | | |
| | −62.3 | 110.0 | | | | |
| | −61.1 | 133.7 | −83.7/−79.5 | 5.3 | 38 | 1.4 |
| | −60.0 | 88.0 | | | | |
| PT-3763 | −65.4 | 89.0 | | | | |
| | −58.3 | 123.0 | −85.5/−82.1 | 4.1 | 26 | 1.4 |
| | −65.7 | 106.3 | −89.2/−80.8 | 10.5 | 26 | 1.3 |
| | −54.8 | 86.9 | −77.1/−72.8 | 5.8 | 28 | 1.4 |
| | −61.1 | 69.8 | −87.8/−85.4 | 6.3 | 16 | 1.8 |
| GSK1034702 | −62.9 | 194.5 | −96.8/−85.7 | 12.9 | 28 | 1.6 |
| | −60.4 | 178.4 | −99.4/−93.8 | 5.9 | 32 | 2.2 |
| | −58.9 | 134.5 | −80.3/−76.5 | 4.9 | 24 | 3.3 |
| | −60.8 | 225.6 | −104.5/−97.3 | 7.3 | 36 | 2.2 |
| | −62.3 | 152.3 | −92.4/−87.4 | 5.8 | 30 | 1.7 |
| | −61.5 | 210.8 | −101.9/−95.4 | 6.8 | 42 | 2.3 |
| | −65.0 | 178.1 | −94.5/−89.4 | 5.7 | 36 | 1.4 |
| | −63.0 | 159.1 | −89.2/−84.4 | 5.6 | 26 | 4.4 |
| | −59.3 | 165.6 | −92.8/−86.4 | 7.4 | 32 | 2.3 |
| | −60.5 | 163.9 | −89.4/−80.8 | 10.7 | 34 | 2.7 |
| Interneurons (putative PV+) | −51.6 | 66.5 | −65.9/64.9 | 1.6 | 198 | 1.3 |
| | −70.6 | 182.5 | −110.7/−107.1 | 3.4 | 42 | 1.6 |
| | −58.5 | 71 | −73.7/−72.7 | 1.5 | 19 | 1.0 |
| | −57.5 | 110.5 | −80.5/−79.6 | 1.2 | 76 | 1.2 |

response was calculated by averaging across all channels that demonstrated a significant increase from baseline firing rate during any drug administration epoch. For each compound tested, data from each slice were used to find the best fit to a four-parameter dose response function as described above for fSP data. A drug-induced increase in spontaneous firing rates was considered significant if the upper asymptote estimate was $>0$ with $p<0.05$. Upper asymptote values were compared across drugs using pairwise *t*-tests, *p* values were corrected using false discovery rate procedure, and differences are reported as significant for corrected *p* values $<0.05$.

For whole-cell recordings of excitatory postsynaptic currents (EPSCs), stimulation artifacts were removed, and data were smoothed by lowpass filtering (cutoff: 500 Hz). Trials in which spikes occurred in voltage clamp following electrical stimulation were discarded, and the mean evoked response was computed across the remaining trials. The maximum negative-going amplitude of the mean evoked EPSC was found, and the initial slope of the EPSCs was defined as the change in current in the initial 10 ms following stimulation. In text and figures, all amplitude, slope, and paired pulse ratio (PPR) data are presented normalized to responses recorded during baseline recording conditions (ACSF + 100 μM picrotoxin) for each cell; raw amplitudes of the evoked EPSCs for each recorded cell are presented in Tables 2 & 3. Statistical analysis was performed in R using a linear mixed effects model (Bates, Maechler, Bolker, & Walker, 2015) with bath, drug

**TABLE 2** Raw maximum negative-going amplitudes of EPSCs (absolute change from prestimulus current value, in pA) evoked by Schaffer collateral and temporoammonic stimulation for pyramidal neurons included in M4-PAM whole cell experiments shown in Figure 3

| | Schaffer collateral | | | | Temporoammonic | | | |
|---|---|---|---|---|---|---|---|---|
| | 100 μM Picrotox | +20 nM Oxotrem. | +1 μM M4 PAM | +3 μM Pirenz. | 100 μM Picrotox | +20 nM Oxotrem. | +1 μM M4 PAM | +3 μM Pirenz. |
| PT-1148 | | | | | 32.8 | 36.7 | 21.0 | |
| | 18.1 | 25.3 | 3.4 | | 39.4 | 58.3 | 49.7 | |
| | 30.2 | 12.6 | 3.5 | | 115.1 | 141.5 | 82.9 | |
| | 31.5 | 43.0 | 39.7 | | 120.9 | 118.4 | 128.8 | |
| | 65.0 | 78.9 | 23.9 | | 111.6 | 117.6 | 48.2 | |
| | 67.7 | 118.6 | 107.1 | | 98.8 | 151.1 | 192.9 | |
| | 84.4 | 115.8 | 14.2 | 46.3 | 37.8 | 69.3 | 32.9 | 74.5 |
| | 146.6 | 116.6 | 40.6 | | 261.7 | 271.3 | 219.1 | |
| PT-3763 | 63.8 | 149.5 | 18.7 | 58.6 | 139.3 | 196.0 | 70.1 | 219.2 |
| | 77.7 | 243.7 | 33.1 | 117.2 | 78.3 | 240.2 | 117.7 | 184.7 |
| | 80.5 | 88.8 | 12.2 | 46.3 | 138.2 | 190.7 | 64.8 | 122.2 |
| | 110.2 | 66.1 | 22.5 | 91.0 | 91.3 | 35.1 | 17.3 | 60.7 |
| | 202.1 | 168.3 | 28.7 | 270.4 | 47.1 | 42.7 | 21.6 | 21.0 |

treatment, and their interaction as fixed factors and cell number as random factor. Least-squares means for specified factors were estimated using the "lsmeans" library (Lenth, 2016). False discovery rate method was used to correct for multiple hypothesis testing. All statistical tests were performed two-tailed at a 5% level of significance.

Firing rates following current injections were determined using standard threshold crossing method to detect evoked spikes and the number of evoked spikes detected was then divided by the 0.5 s pulse duration. For pyramidal cells, spike rates evoked by a 200 pA current pulse were analyzed for all cells; for putative interneurons, the current step used for analysis was determined separately for each cell as the lowest step that evoked a firing rate of $>30$ Hz under baseline conditions (step amplitudes = 100–300 pA). For the pyramidal cells, spike frequency adaptation was measured by first quantifying inter-spike intervals (ISIs) for each action potential elicited by a 200 pA current injection for each cell and bath condition. Table 1 presents the ratio of the $5^{th}$ ISI to the $1^{st}$ ISI at baseline conditions for each cell. Statistical analysis of the ISI growth curves was performed using a linear mixed effects model in R, with spike number and bath as fixed factors and cell number as the random factor. Post-hoc analyses were performed using the same model to compare baseline to GSK1034702 and baseline to pirenzipine conditions. Spike number, bath, and interaction terms were considered statistically significant if false discovery rate adjusted $p < 0.05$.

**TABLE 3** Raw maximum negative-going amplitudes of EPSCs (absolute change from prestimulus current values, in pA) evoked by Schaffer collateral and temporoammonic stimulation for pyramidal neurons included in the GSK1034702 experiments shown in Figure 5

| | Schaffer collateral | | | Temporoammonic | | |
|---|---|---|---|---|---|---|
| GSK-702 | 100 μM Picrotox | +300 nM GSK | +3 μM Pirenz. | 100 μM Picrotox | +300 nM GSK | +3 μM Pirenz. |
| | 71.7 | 88.8 | 105.0 | | | |
| | 65.8 | 61.9 | 46.7 | | | |
| | 102.4 | 59.4 | 82.3 | | | |
| | 56.3 | 79.6 | 40.0 | 83.0 | 93.2 | 73.8 |
| | 58.4 | 121.4 | 41.3 | 38.7 | 61.0 | 80.8 |
| | 64.0 | 71.0 | 39.2 | 40.9 | 72.6 | 103.7 |
| | 61.5 | 77.6 | 139.8 | 56.3 | 89.1 | 188.8 |
| | 78.1 | 71.1 | 30.8 | 56.8 | 81.4 | 68.1 |
| | 102.6 | 80.7 | 98.1 | 42.7 | 25.2 | 48.8 |
| | 121.9 | 92.8 | 69.2 | 119.2 | 139.5 | 134.5 |

**TABLE 4** Selectivity of the M4 activators used in this study

| | PT-1148 | | PT-3763 | | PT-6950 | |
|---|---|---|---|---|---|---|
| | EC50 (nM) | E-max (%) | EC50 (nM) | E-max (%) | EC50 (nM) | E-max (%) |
| hM1 | - | - | - | - | 312 [124–780] | 8.1 [6.1–10.3] |
| hM2 | 1,609 [863–2,998] | 100.1 [76.7–123.5] | 1,277 [991–1,645] | 206.1* [189.4–222.9] | 2,879 [324–25,920] | 107.2 [16.7–197.7] |
| hM3 | - | - | - | - | - | - |
| hM4 | 3.0 [1.74–5.01] | 93.8 [91.4–96.2] | 45 [39–50] | 123.1* [120.2–126.0] | 20 [16–25] | 99.5 [96.0–102.9] |
| hM5 | - | - | - | - | - | - |
| rM4 | 0.46 [0.062–3.36 | 101.9 [99.54–104.3] | 0.81 [0.007–9.2] | 129.7* [111.8–147.5] | 2.62 [2.24–3.06] | 109.1 [107.9–110.3] |

Compounds were tested for functional response at the five human muscarinic receptor subtypes (hM1–hM5) and at rat M4 (rM4) receptors. E-max values for each compound are expressed as a percentage of the response of a saturating concentration of ACh (10 μM). Assays were run using the compound alone (agonist mode) for PT-6950 and in the presence of an EC20 of ACh (PAM mode) for PT-1148 and PT-3763. ACh EC20 values for different cell lines were hM1 = 5 nM, hM2 = 3 nM, hM3 = 0.8 nM, hM4 = 15 nM, hM5 = 2 nM, and rM4 = 0.8 nM. Dashes (-) denote E-max values not significantly different from 0%, or EC50 values >10,000 nM; brackets contain 95% confidence intervals. * PT-3763 E-max results may be confounded by known antagonism of beta-2 adrenergic receptors, which were stimulated with isoproterenol to increase cAMP in M2 and M4 functional selectivity experiments (see Methods)

### 2.6 | In vitro muscarinic functional activity

To verify the selectivity of the muscarinic compounds used in this study, we tested the functional activity of GSK1034702, PT-1148, PT-3763, and PT-6950 in six different cell lines, each stably expressing a different human muscarinic receptor subtype (hM1-hM5) or the rat M4 receptor (rM4). All selectivity screening was performed at Pfizer (La Jolla, CA) and HD Biosciences Co., Ltd. (Shanghai, China). M2 and M4 mAChR activity was evaluated using GloSensor™ cAMP detection technology (Promega, Madison, WI). hM2, hM4, and rM4 expressing HEK293 stable cell lines were generated from a host cell line stably expressing the GloSensor™. M2 and M4 mAChRs are $G_{i/o}$-coupled and their activation is associated with a decrease in cAMP (Wess, 1996). To elevate an otherwise low cellular cAMP level, cells were treated with an EC80 concentration of isoproterenol (50 nM), which is an agonist of endogenously expressed beta-2 adrenergic receptors, $G_s$-coupled receptors known to raise intracellular cAMP (Rasmussen et al., 2011).

M1, M3, and M5 mAChRs are $G_{\alpha q}$-coupled GPCRs that activate phospholipase C (PLC), which hydrolyzes phosphatidylinositol bisphosphate ($PIP_2$) to form two second messengers: inositol 1,4,5-triphosphate ($IP_3$) and DAG. $IP_3$ then activates the $IP_3$ receptor on the endoplasmic reticulum (ER) resulting in an elevation of intracellular $Ca^{2+}$ (Berridge, 1993). FLIPR™ (Molecular Devices, Sunnyvale, CA) was used to quantify $Ca^{2+}$ release induced by the muscarinic compounds in CHO K1 cell lines stably expressing hM1, hM3, or hM5 receptors.

In all plate-based experiments, the effect of each compound is expressed as a percentage of the response generated by a saturating concentration of ACh (10 μM) included on each plate. The PAMs PT-1148 and PT-3763 were tested for functional activity in the presence of an EC20 concentration of ACh, determined separately for each cell line. The ACh EC20 values for each cell line were as follows: hM1: 5 nM; hM2: 3 nM; hM3: 0.8 nM; hM4: 15 nM; hM5: 2 nM; rM4: 0.8 nM. *In vitro* dose–response data from replicate experiments ($n > 3$) was analyzed using GraphPad Prism to find the best fits to a four parameter logistic function. For each compound and muscarinic receptor subtype, EC50 and E-max values are reported along with 95% confidence intervals (Table 4).

To further characterize the selectivity of each compound, additional GloSensor, FLIPR, or MicroBeta radiometric (PerkinElmer, Waltham MA) assays were run to quantify functional activity at a number of nonmuscarinic receptors, amine transporters, ion channels, and phosphodiesterases. Significant nonmuscarinic activity was rarely found for the M1- and M4-selective compounds used in this study, and where off-target activity was observed, IC50 values are reported in the Results.

## 3 | RESULTS

### 3.1 | PT-1148, PT-3763, and PT-6950 are potent and specific M4 activators

Three recently developed compounds were used in this study to selectively activate M4 receptors, the first use of these compounds in native tissue, to our knowledge. These included two PAMs, PT-1148 (Lindsley et al., 2013) and PT-3763 (Brady et al., 2008; Lindsley et al., 2013), and a putative bitopic agonist, PT-6950 (Livermore et al., 2014). Using GloSensor™ and FLIPR™ assays, we tested the functional selectivity of each of these compounds for the hM4 receptor compared to the other mAChRs (Figure 1 and Table 4), and for activity at a number of nonmuscarinic receptors and phosphodiesterases (data not shown). Because M4 receptors in rats and humans are known to differ in their amino acid sequences and thus likely to interact differently with various ligands, we additionally tested the functional activity of the compounds at rM4 receptors. All three M4 activators were selective for the hM4 and rM4 receptors over other neurotransmitter receptors and phosphodiesterases (Table 4). PT-1148 exhibited the greatest selectivity, potently potentiating hM4 (PAM EC50 = 3 nM) and exhibiting no significant activation at any other receptors examined except hM2 (PAM EC50 = 1,609 nM, 536-fold shift). PT-3763 was less selective for hM4 over hM2, reaching half-maximal receptor potentiation at

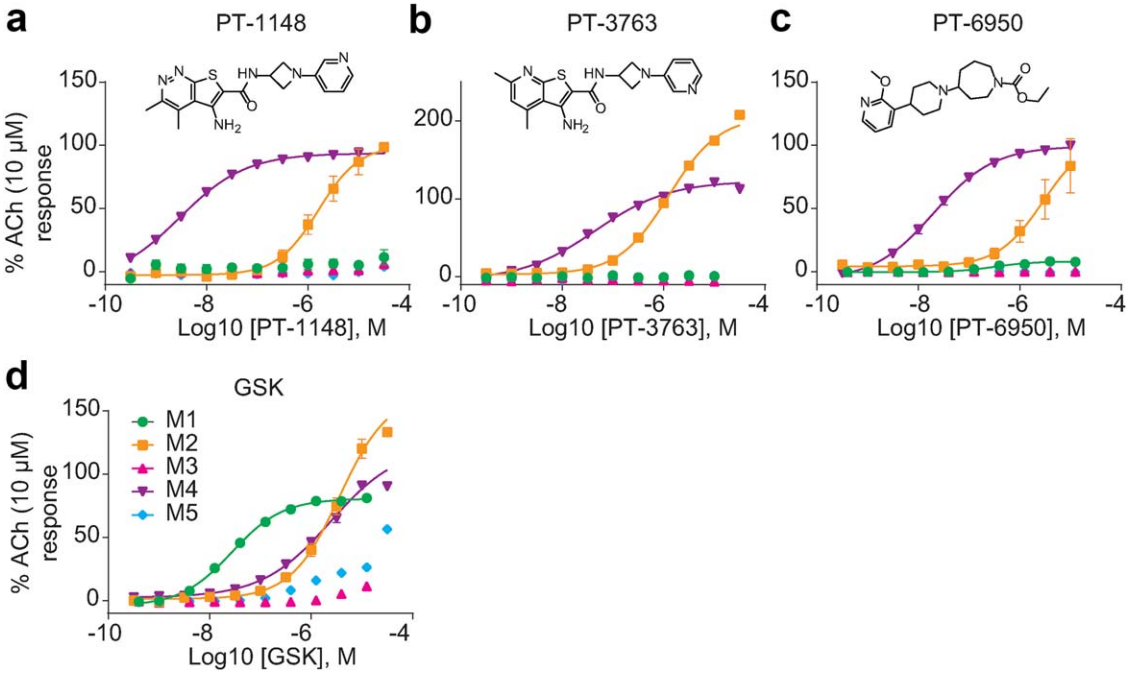


**FIGURE 1** PT-1148, PT-3763, and PT-6950 selectively activate M4 receptors, and GSK1034702 (GSK) selectively activates M1 receptors. (**a–d**) PT-1148 (a), PT-3763 (b), PT-6950 (c), and GSK1034702 (d) were tested for functional response at each of the human muscarinic receptor subtypes utilizing FLIPR$^{TM}$ (for M1, M3, and M5) or GloSensor$^{TM}$ (for M2 and M4)-based assays to quantify muscarinic-mediated increases in intracellular calcium or decreases in cAMP, respectively. Insets in (a–c) illustrate the chemical structures for previously unpublished M4 compounds. Legend for all panels shown in (d). Positive allosteric modulators (PAMs) PT-1148 and PT-3763 were tested in the presence of an EC20 concentration of ACh: $EC20_{M1} = 5$ nM, $EC20_{M2} = 3$ nM, $EC20_{M3} = 0.8$ nM, $EC20_{M4} = 15$ nM, $EC20_{M5} = 2$ nM [Color figure can be viewed at wileyonlinelibrary.com]

45 nM for hM4 and 1277 nM for hM2 (28-fold shift). PT-3763 also antagonized beta-2 adrenergic receptors at higher concentrations (IC50: 2,990 nM). The agonist PT-6950 was also highly selective for hM4 receptors over other mAChRs. It acted as a potent full agonist at hM4 (EC50 = 20 nM), a much less potent full agonist at hM2 (EC50 = 2,879 nM), and a very low partial agonist at hM1 (EC50 = 312 nM, but maximal activation only 8% relative to ACh). This compound was therefore 143-fold more potent at our hM4 cell line compared to our hM2 cell line. When we account for the fact that our hM2 cell line was 3 times more sensitive to ACh than our hM4 cell line (ACh EC50 13 nM for hM2 compared to 40 nM for hM4), the corrected hM4:hM2 selectivity ratio for PT-6950 is more than 400-fold (Kenakin, Watson, Muniz-Medina, Christopoulos, & Novick, 2012). PT-6950 also displayed some antagonist activity at A1a receptors (IC50: 552 nM) and 5HT2b receptors (IC50: 1,260 nM).

To compare the new M4 compounds to previously existing tools, we evaluated the *in vitro* selectivity of the M4 PAM compounds LY2033298 (Nawaratne et al., 2008) and VU152100 (Brady et al., 2008). LY2033298 potentiated hM4 with an EC50 of 41 nM, and hM2 with an EC50 of 3,276 nM, an 80-fold difference. VU152100 was much weaker in our assays and less selective ($hM4_{EC50}$: 817 nM, $hM2_{EC50}$: 8,701 nM). The three newer compounds therefore exhibit selectivity profiles comparable to or better than those of existing M4 activators. In addition, while LY2033298 is much weaker at the rat M4 receptor than the human (Chan et al., 2008), all three new M4 activators exhibited more potent activation of rM4 receptors compared to hM4 receptors (PT-1148: $rM4_{EC50}$: 0.46 nM; PT-3763: $rM4_{EC50}$: 0.81 nM; PT-6950: $rM4_{EC50}$: 2.62 nM), making them very good research tools for use in rat studies.

We used the previously published compound GSK1034702 to selectively activate M1 receptors for these experiments (Nathan et al., 2013; Ridler et al., 2014). Using the same FLIPR$^{TM}$ and GloSensor$^{TM}$ assays as above, we confirmed that this compound is reasonably selective for hM1 (Figure 1; EC50: 27 nM; E-max: 80.8% of ACh E-max) over the other mAChRs, with hM4 being the next most activated (hM4 EC50: 1,427 nM; hM4 E-max: 122.4% of ACh E-max).

## 3.2 | M4 activation powerfully reduces glutamatergic synaptic transmission in the SC pathway

Previous studies have shown that muscarinic activation dramatically decreases synaptic transmission in the SC pathway (Cea-del Rio et al., 2010; Dasari & Gulledge, 2011; Easton et al., 2012; Fernandez de Sevilla & Buno, 2003; Hasselmo & Schnell, 1994; Hounsgaard, 1978; Qian & Saggau, 1997; Shirey et al., 2008; Valentino & Dingledine, 1981). Consistent with these prior reports, the muscarinic agonist oxotremorine dose dependently reduced field potentials evoked by electrical stimulation of axons in the stratum radiatum (Figure 2a) to approximately 12% of their initial amplitude (12.2 ± 8.2%, mean ± SEM). Blocking M1 receptors with VU0255035 resulted in a small but

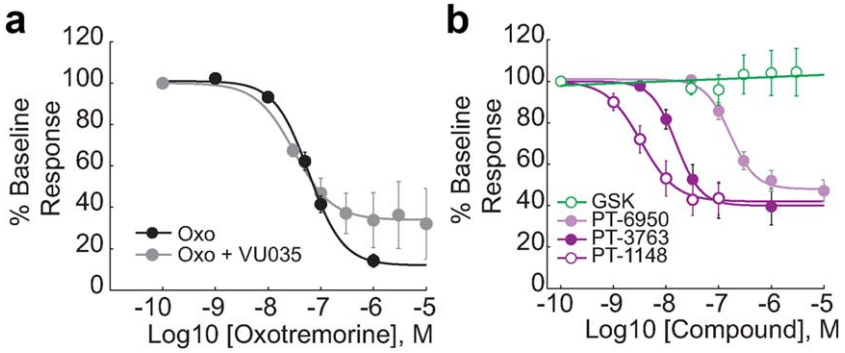


**FIGURE 2** Selective activation of M4 ACh receptors strongly suppresses synaptic transmission in the SC pathway. (**a**) The pan-muscarinic agonist oxotremorine (Oxo) produces a concentration-dependent reduction in the amplitude of extracellular field potentials evoked by electrical stimulation of SC axons in the stratum radiatum, with a maximum reduction to approximately 12% of baseline amplitudes. Blocking M1 receptors with VU0255035 (VU035, 1 μM) results in a small decrease in the maximum suppression produced by oxotremorine (to 33.5% of baseline). (**b**) The M4 PAMs PT-1148 and PT-3763, and the M4 agonist PT-6950, also produce a concentration-dependent reduction in SC stimulation evoked field potential amplitudes, with a maximum reduction to approximately 40% of baseline amplitudes. The M1 agonist GSK1034702 (GSK) has no significant effect on the amplitude of field potentials evoked by SC stimulation [Color figure can be viewed at wileyonlinelibrary.com]

significant reduction in the maximal suppression of the evoked field potentials by oxotremorine (to 33.5 ± 5.1%, OXO vs. OXO + VU0255035: $p = 0.034$, false discovery rate corrected pairwise *t*-test).

To assess the involvement of M4 receptors in mediating this suppression, we tested the effects of the selective M4 PAMs PT-1148 and PT-3763 in the same assay. Because these compounds do not directly activate the M4 receptor, but rather act at an allosteric site to potentiate the binding of an orthosteric ligand, we tested these M4 PAMs in the presence of an EC20 concentration of oxotremorine, which was determined from the fitted dose–response curve shown in Figure 2a ($EC20_{oxo} = 20$ nM). To ensure that oxotremorine was not required for the observed effects, the M4 agonist PT-6950 was additionally tested, in the absence of oxotremorine. All three M4 activators strongly and dose dependently reduced the amplitude of the evoked field response (Figure 2b), though with a maximum reduction to approximately 40% of baseline amplitudes ($OXO_{EC20}$+PT-3763: 39.9 ± 5.0%; $OXO_{EC20}$+PT-1148: 41.7 ± 6.4%, PT-6950: 48.4 ± 4.7%; mean ± SEM), the effect of M4 activation was not as powerful as that observed for oxotremorine ($OXO_{EC100}$ vs. $OXO_{EC20}$+PT-3763: $p = .0054$; $OXO_{EC100}$ vs. $OXO_{EC20}$+PT-1148: .0054; $OXO_{EC100}$ vs. $OXO_{EC20}$+PT-6950: .0006; false discovery rate corrected pairwise *t*-tests). The maximum reductions in fSP amplitude for the M4 PAMs PT-1148 and PT-3763 are reported relative to the fSP amplitude following the application of an EC20 of oxotremorine, and this reduced baseline may contribute to an underestimation of the effect size for these two compounds. However, a 20% lower baseline amplitude is unlikely to fully account for the observed difference in maximal efficacy between oxotremorine and the M4 PAMs.

By contrast to the M4 activators, the selective M1 allosteric agonist GSK1034702 failed to reduce SC-evoked field potential amplitudes at any concentration tested (Figure 2b). Combined, these results suggest that activation of M4 receptors robustly reduces evoked synaptic transmission in the SC pathway, though other mAChRs are likely to additionally contribute to the suppression of SC synapses. In particular, while GSK1034702 did not significantly suppress SC-evoked field potentials, we cannot rule out some involvement of M1 receptor activation in contributing to the suppressive effects of oxotremorine.

We next used whole-cell patch clamp recordings from single CA1 pyramidal neurons to examine the M4-mediated reduction in evoked synaptic transmission in more detail, and to ask whether M4 activation differentially affects transmission in the SC and TA pathways. For these experiments, 100 μM picrotoxin was bath applied to block GABA-A receptors and isolate synaptic activity in the excitatory pathways. The effects of M4 activation were tested using both PT-3763 (1 μM) and PT-1148 (1 μM) at concentrations that produced maximal responses in the field potential studies. Using a linear mixed effects statistical model with a fixed effect for the specific M4 PAM applied, no significant difference between the effects of PT-3763 and PT-1148 on the amplitude or slope of the SC or TA evoked EPSCs was found ($p_{SC,amp} = 0.658$, $p_{SC,slope} = 0.557$, $p_{TA,amp} = 0.844$, $p_{TA,slope} = 0.650$). Thus, the data from these two compounds were combined for all subsequent analyses.

In whole-cell recordings in the presence of picrotoxin (PTX, 100 μM) and a low concentration of oxotremorine (OXO, 20 nM), M4 PAMs (M4, 1 μM) produced a dramatic reduction in the amplitude (to 43.2 ± 13.7% of response in PTX alone, mean ± SEM; PTX + OXO vs. PTX + OXO + M4: $p = .0003$, FDR-adjusted post-hoc pairwise comparison) and slope (to 16.6 ± 3.6% of baseline, PTX + OXO vs. PTX + OXO + M4: $p = .0006$) of EPSCs evoked by SC stimulation (Figure 3a–c), and this effect was reversed by the application of the muscarinic antagonist pirenzepine (3 μM). In the same cells, M4 activation also produced a significant decrease in TA-evoked EPSC amplitudes (to 83.8 ± 13.7% of baseline; PTX + OXO vs. PTX + OXO + M4: $p = .0037$) and slopes (to 68.1 ± 12.3% of baseline; PTX + OXO vs. PTX + OXO + M4: $p = .0004$), but the magnitude of this decline was significantly smaller at TA synapses than at SC synapses (BATH × PATHWAY interaction: $p = 0.047$; SC vs. TA post-hoc comparison: $p = 0.0172$).

Consistent with a presynaptic decrease in neurotransmitter release, M4 activation significantly increased paired pulse facilitation in

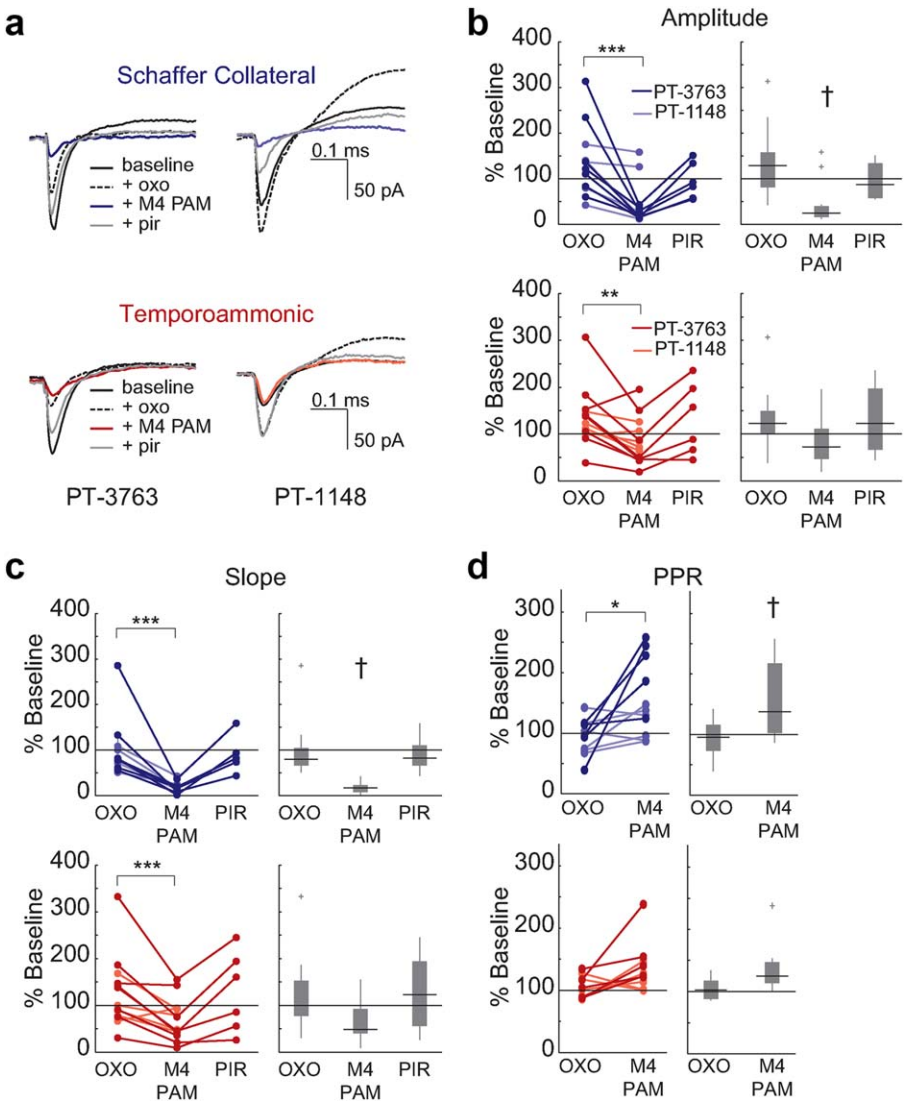


**FIGURE 3** M4 activation exhibits differential presynaptic suppression of synaptic transmission in SC and TA pathways. (**a**) Sample EPSC traces following stimulation of either SC (top) or TA (bottom) axons during sessions in which PT-3763 (left) or PT-1148 (right) were applied. (**b,c**) M4 activation with PT-1148 (light lines) or PT-3763 (dark lines) produces a stronger suppression of EPSC amplitudes (b) and slopes (c) produced by SC (blue, top) compared to TA (red, bottom) stimulation; suppression is reversed following application of the muscarinic antagonist pirenzipine (PIR). (**d**) Paired pulse ratios (PPR) are significantly increased following M4 activation in the SC (blue, top), but not TA (red, bottom) pathway. * $p < .05$, ** $p < .01$, *** $p < .001$, false discovery rate corrected post-hoc pairwise comparison; † significant difference from baseline response with $p < .05$, one-way ANOVA. Baseline recordings were performed in ACSF with 100 μM picrotoxin. OXO = oxotremorine (20 nM); M4 PAM = PT-1148 or PT-3763 (1 μM); PIR = pirenzipine (3 μM) [Color figure can be viewed at wileyonlinelibrary.com]

the SC pathway to 156.8 ± 18.9% (mean ± SEM) of baseline values (Figure 3d; PTX + OXO vs. PTX + OXO + M4: $p = .022$, FDR-adjusted post-hoc comparison). At TA synapses, activation of M4 receptors again exhibited reduced effectiveness, producing a trend toward increased PPRs (to 136.3 ± 12.6% of baseline, mean ± SEM) that failed to reach statistical significance ($p = .068$). Following the whole-cell experiments with PT-3763, we verified that the recorded EPSCs were driven by synaptically evoked glutamate release using the AMPA/kainate receptor antagonist CNQX (5 μM) to suppress SC- and TA-evoked responses (mean ± SEM of CNQX-induced suppression from end of recordings: SC = 85.2 ± 4.1%; TA = 79.4 ± 4.8%). Combined, our results show that specific activation of M4 receptors powerfully reduces glutamatergic signaling in SC pathway while leaving TA synaptic transmission comparatively intact. These results further suggest that the most likely mechanism for this effect is through activation of presynaptic M4 receptors on SC terminals. M4 immunoreactivity in CA1 was observed to be highest in the stratum radiatum, and associated with noncholinergic fibers (Levey et al., 1995). Moreover, M4 mRNA is expressed in rat CA3 pyramidal neurons (Buckley, Bonner, & Brann, 1988), which give rise to the Schaffer collateral axons. Here, we find a simultaneous reduction in the CNQX-sensitive EPSC amplitude and an increase in paired pulse facilitation resulting from M4 activation, results

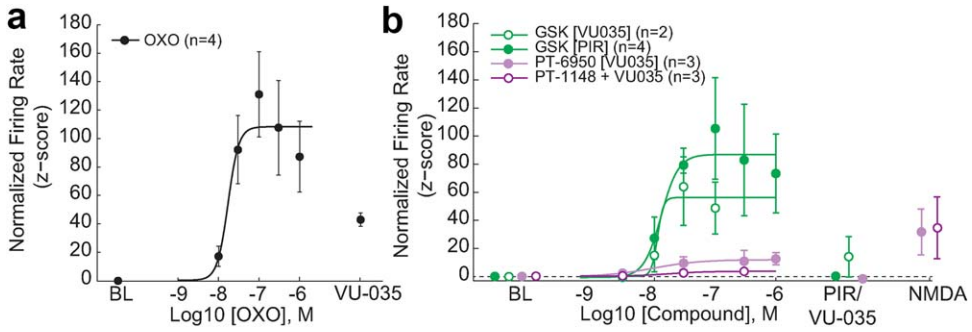


**FIGURE 4** M1 activation increases spontaneous firing rates in hippocampal CA1 slices. (**a**) Oxotremorine (OXO) produces a concentration-dependent increase in CA1 firing rates that is only partially reversed by the M1 antagonist VU0255035 (1 μM). (**b**) Specific M1 activation with GSK1034702 (green) also produces a concentration-dependent increase in spontaneous firing rates in CA1, which can be reversed with the muscarinic antagonist pirenzipine (3 μM, closed circles) and with the specific M1 antagonist VU0255035 (1 μM, open circles). M4 activation with the PAM PT-1148 (dark purple) in the presence of 20 nM oxotremorine and 1 μM VU0255035 did not significantly increase CA1 firing rates, nor did M4 activation with the agonist PT-6950 (light purple). [Color figure can be viewed at wileyonlinelibrary.com]

which point to an M4-mediated reduction of presynaptic glutamate release. While the M4-selective compounds were not as effective as oxotremorine, their effect sizes do indicate that M4 activation is sufficient to explain a major portion of the differential suppressive effect of acetylcholine at SC versus TA synapses (Hasselmo & Schnell, 1994).

### 3.3 | M1 activation increases intrinsic excitability of CA1 pyramidal neurons without affecting excitatory synaptic inputs

Activation of M1 receptors has been shown to increase the intrinsic excitability of a variety of cell types, including CA1 pyramidal neurons (Bell, Bell, & McQuiston, 2015b; Dasari & Gulledge, 2011; Fisahn et al., 2002; Weiss et al., 2000; Xiang, Thompson, Jones, Lindsley, & Conn, 2012; Yi et al., 2014). Spontaneous firing rates can provide an indirect indication of neuronal excitability in both *in vivo* and *in vitro* preparations. In extracellular recordings of spontaneous firing rates in hippocampal slices from adult rats, we confirmed that oxotremorine produced a concentration-dependent increase in the *z*-score normalized spontaneous firing rates of CA1 neurons (Figure 4a, upper *z*-score asymptote = 108.2 ± 6.3, mean ± SEM; $p < 0.0001$), and this effect was partially reversed by 3 μM of the M1-selective antagonist VU0255035 (Sheffler et al., 2009). The M1-selective agonist GSK1034702 was also found to dose-dependently increase CA1 firing rates (upper *z*-score asymptote, GSK1034702 with pirenzipine reversal = 86.9 ± 13.6, $p < 0.0001$; upper *z*-score asymptote, GSK1034702 with VU0255035 reversal = 56.3 ± 11.9, $p < 0.0001$), and this effect was reversed by both the muscarinic antagonist pirenzepine (3 μM) and the more specific M1 antagonist VU0255035 (3 μM; Figure 4b). By contrast, the M4 PAM PT-1148, in the presence of 20 nM oxotremorine and 1 μM VU0255035, did not significantly increase CA1 firing rates at any concentration tested (Figure 4b; upper *z*-score asymptote = 3.77 ± 23.9, $p = 0.875$). The M4 agonist PT-6950 also failed to produce a significant increase in CA1 spike rates (upper *z*-score asymptote = 12.0 ± 16.7, $p = 0.474$). We found a significant difference between asymptotic normalized spike rates evoked by GSK1034702 and the two M4 activators (GSK1034702 vs. PT-1148: $p = 0.0167$; GSK1034702 vs. PT-6950: $p = 0.0070$, FDR corrected pairwise comparison), and between spike rates evoked by the M1 agonist GSK1034702 and oxotremorine (GSK1034702 vs. OXO: $p = 0.0176$, FDR-adjusted pairwise comparison). Combined, these results suggest that the observed muscarinic-mediated increases in CA1 pyramidal cell firing rates are largely due to the activation of M1, and not M4, receptors. Other mAChRs are likely to additionally contribute to ACh-mediated spike rate increases, however, as oxotremorine produced significantly higher firing rates than GSK1034702 and VU0255035 only partially reversed the firing rate increases produced by oxotremorine.

Increased spontaneous firing could be mediated by increases in intrinsic excitability of CA1 neurons, or by enhanced glutamatergic excitation by SC and/or TA inputs. In whole cell recordings, GSK1034702 had no significant effect on the amplitude, slope, or PPR of EPSCs evoked by stimulation of either the SC or TA pathways (Figure 5a–d, top; SC amp: $p = 0.46$, SC slope: $p = 0.57$, SC PPR: $p = 0.54$, TA amp: $p = 0.15$, TA slope: $p = 0.089$, TA PPR: $p = 0.78$, FDR-adjusted post-hoc pairwise comparisons). Combined with the similar results obtained during extracellular recordings (Figure 2b), these results suggest that for both SC and TA synapses, M1 activation with GSK1034702 does not significantly impact the release of glutamate from presynaptic terminals, the number of AMPA receptors expressed postsynaptically, or the level of activation of existing AMPA receptors.

Consistent with an M1-mediated increase in intrinsic excitability, GSK1034702 did increase the number of spikes evoked in response to a 200 pA injected current step (Figure 5e; Baseline vs. GSK1034702: $p = 0.012$, FDR-adjusted post-hoc pairwise comparison), and this effect was reversed with pirenzepine (3 μM; Baseline vs. pirenzipine: $p = 0.28$, FDR-adjusted post-hoc comparison). Moreover, spike frequency accommodation was significantly reduced among CA1 pyramidal cells following application of GSK1034702, and this effect was similarly reversed with pirenzipine (Figure 5f). Specifically, a mixed

linear effects model examining the effect of both spike number within the evoked spike train as well as drug condition on the interspike intervals revealed significant effects of spike number and the interaction of drug and spike number, but no significant effect of drug condition alone (spike number: $p = 2.2e\text{-}16$; drug effect: $p = 0.12$; interaction: $p = 0.0004$). Post-hoc modeling comparing baseline recordings to GSK1034702 and pirenzipine recordings demonstrated significant drug and interaction effects of GSK1034702 (Baseline vs. GSK1034702, spike number: $p = 2.2e\text{-}16$; drug effect: $p = 0.0013$; interaction: 6.4e-9) but not pirenzipine (Baseline vs. pirenzipine, spike number: $p = 2.0e\text{-}16$; drug effect: $p = 0.20$; interaction: $p = 0.91$). These results suggest that the ACh-mediated increases in intrinsic excitability can be recapitulated by selective M1 activation.

Following M1 activation, increases in excitability were also observed for a small population of putative PV+ CA1 interneurons recorded ($n = 4$). All interneurons showed increased firing rates following the application of GSK1034702 (Figure 5g; $p = 0.0275$, paired single-tail *t*-test). These data support previous findings pointing to the presence of M1 receptors on PV+ CA1 cells (Yi et al., 2014) and suggest that increased feedforward inhibition is one potential mechanism by which enhanced pyramidal cell excitability may remain balanced in the intact network following M1 activation.

Taken together, our results suggest that targeted activation of M1 and M4 receptors is sufficient to reproduce the major actions of ACh on CA1 excitatory synaptic transmission (Figure 6). Activation of postsynaptic M1 receptors increases the excitability of CA1 pyramidal neurons and interneurons, without significantly altering evoked EPSC amplitudes in either the SC or TA pathways. Activation of presynaptic M4 muscarinic receptors dramatically dampens SC synaptic input while producing less pronounced effects on TA synaptic transmission. Combined, these findings support a conceptual framework in which increased cholinergic tone, or selective activation of M1 and M4 receptors, can bias the hippocampal CA1 network toward entorhinal cortical inputs and memory encoding functions.

## 4 | DISCUSSION

Using selective pharmacological manipulation of M1 and M4 receptors in hippocampal CA1, we have demonstrated that activation of these two specific receptor subtypes is sufficient to reproduce several of the major effects previously reported for ACh. Specifically, activation of M1 receptors increases intrinsic excitability, decreases spike frequency accommodation, and increases spontaneous firing rates of CA1 pyramidal neurons and GABAergic interneurons, while exerting only minor effects on evoked synaptic transmission in either the SC or TA pathways. By contrast, activation of M4 receptors dramatically reduced evoked synaptic responses in the SC pathway, likely by acting to decrease presynaptic transmitter release at the glutamatergic SC synapses, while leaving the TA pathway synapses comparatively uninhibited. Using several previously unpublished M4-selective compounds, our results demonstrate that M4 activation likely mediates the differential suppressive effect of acetylcholine at SC and TA synapses previously reported by Hasselmo and Schnell (1994). A role for M4 in mediating this effect is further supported by the immunohistochemical findings of Levey et al. (1995) demonstrating much greater M4 receptor expression in the stratum radiatum, which receives SC input, compared to the stratum lacunosum moleculare, which receives input from the TA pathway. Combined, these results clarify and extend conflicting pharmacological literature (Kremin et al., 2006; Leung & Peloquin, 2010; Sanchez et al., 2009; Seeger & Alzheimer, 2001; Sheridan & Sutor, 1990; Shirey et al., 2008; de Vin et al., 2015) and provide support for similar findings from previous studies using knockout animals (Dasari & Gulledge, 2011). When viewed within the context of the extensive hippocampal literature, the present results are consistent with the hypothesis that muscarinic activation should favor a hippocampal network state conducive to memory encoding.

### 4.1 | Co-activation of SC and TA synapses may be critical for memory encoding

Major models of hippocampal function presume that a specific pattern of CA1 neuron activation represents a specific set of episodic memory features such as the animal's location within a familiar context (Cutsuridis et al., 2010; Hasselmo & Wyble, 1997; Knierim & Neunuebel, 2016; Rolls & Kesner, 2006). This activation pattern can be driven purely by the SC pathway, which represents a processed version of the current sensory experience carried in by the perforant pathway and passed through the dentate-CA3 pattern recognition network (Kesner & Rolls, 2015). Familiar experiences could thus be expected to reliably reactivate a fixed subpopulation of CA1 neurons by virtue of the classical trisynaptic circuitry of the hippocampus. In this context, a novel experience enters the trisynaptic circuit as a distinct activity pattern but the pattern completion functions of the CA3 autoassociative network tend to converge toward pre-existing patterns that represented the most similar past experiences, such that the novelty of the pattern arriving through the SC-CA1 pathway is reduced (Neunuebel & Knierim, 2014). TA inputs, by contrast, more directly convey the novel elements of the experience to CA1, enabling the overall hippocampal output pattern to at least partially reflect the unfamiliar features independently of the trisynaptic loop. This pattern will not be stabilized within the network, however, unless synaptic connections within the trisynaptic loop are modified. During memory encoding, the combination of co-active SC and TA inputs to CA1 can efficiently induce synaptic plasticity through the production of dendritic plateau potentials within a subset of activated CA1 neurons (Kaifosh & Losonczy, 2016; Takahashi & Magee, 2009). This pattern of synaptic activation, and subsequent replay of activity during sleep, is thought to be a key component of successful memory encoding (Abel, Havekes, Saletin, & Walker, 2013; Atherton, Dupret, & Mellor, 2015; Girardeau & Zugaro, 2011; O'Neill, Pleydell-Bouverie, Dupret, & Csicsvari, 2010; Sutherland & McNaughton, 2000).

A number of studies provide support for this basic model. When stimulated alone, TA synapses in adult rat slices are more prone to LTD than to LTP (Dvorak-Carbone & Schuman, 1999). However, these same synapses can be robustly potentiated when paired with an SC

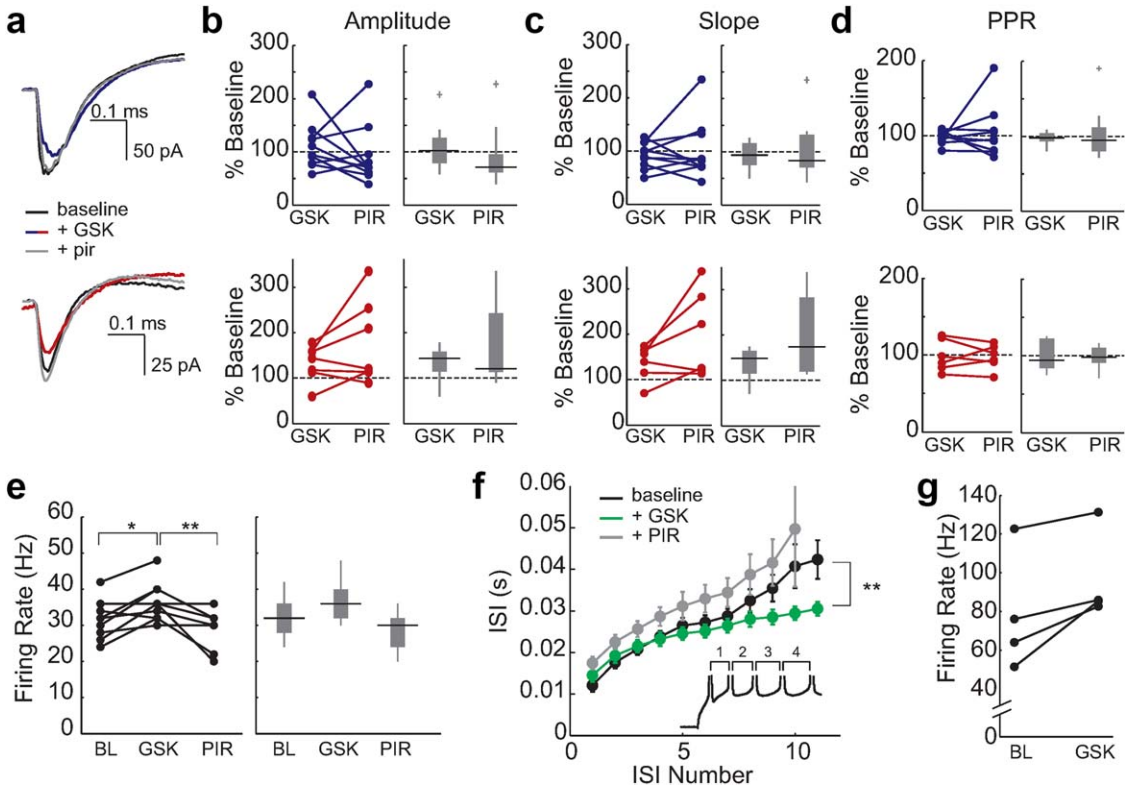


**FIGURE 5** M1 activation increases intrinsic excitability without altering evoked excitatory synaptic transmission in CA1. (**a**) Sample EPSC traces following SC (top) or TA (bottom) stimulation during sessions in which the M1 agonist GSK1034702 was applied. (**b–d**) GSK1034702 does not significantly change the amplitudes (b), slopes (c), or paired-pulse ratios (PPR) (d) of EPSCs evoked by SC (blue, top) or TA (red, bottom) stimulation. (**e**) GSK1034702 increases the firing rates of CA1 pyramidal neurons in response to a 200 pA current injection; responses return to baseline (BL) levels following muscarinic antagonism with pirenzipine; * $p < 0.05$; ** $p < 0.01$, false discovery rate corrected post-hoc pairwise comparison. (**f**) Spike-frequency accommodation is reduced following GSK1034702 application (green) and returns to baseline levels with pirenzipine (gray). Inset: sample trace illustrating interspike intervals (ISIs) and ISI numbers in the 300 ms following current step onset for a single pyramidal neuron during baseline conditions. Baseline recordings were performed in ACSF with 100 μM picrotoxin. GSK = GSK1034702 (300 nM); PIR = pirenzipine (3 μM). [Color figure can be viewed at wileyonlinelibrary.com]

stimulus because the pairing efficiently triggers dendritic plateau potentials (Takahashi & Magee, 2009). These results predict that TA inputs that are regularly paired with SC activation should be strengthened, whereas unpaired TA inputs should be weakened. Highlighting the significance of dendritic plateau potentials for memory encoding, Bittner et al. (2015) recently demonstrated that in CA1 neurons of awake mice, if plateau potentials occurred while the animal was in a location that had not previously been associated with activation of the neuron, that location would rapidly become a new place field for the neuron. This was true whether the plateau potentials occurred spontaneously or were evoked by direct stimulation. This suggests a model whereby specific TA and SC co-activation patterns represent features to be remembered, and when a co-activation pattern successfully results in dendritic plateau potential generation in a CA1 neuron, it will induce plastic changes that specifically strengthen the neuron's response to that input pattern. Bittner et al. (2015) also observed that when the animal moved through a neuron's established place field, dendritic plateau potentials were again frequently observed. This would be expected to further stabilize the neural representation of that location, and to strengthen new associations that form with repeated experiences. Over time, the neuron should respond not only to the exact input pattern but also to partially degraded or incomplete versions of it, enabling the pattern completion function that has long been associated with the hippocampus (Knierim & Neunuebel, 2016; Marr, 1971; O'Reilly & McClelland, 1994; Rolls & Kesner, 2006; Treves & Rolls, 1994).

## 4.2 | M1 and M4 receptors support complementary processes during memory encoding

Under this model, the actions of M1 and M4 receptors on CA1 circuitry appear to support complementary aspects of memory encoding. M1 activators, by boosting postsynaptic excitability and therefore the likelihood of plateau potential generation, may facilitate the strengthening of relatively weak TA and SC input pairings. The direct contributions of M1 receptors to SC LTP (Buchanan et al., 2010; Dennis et al., 2016; Dominguez, Fernandez de Sevilla, & Buno, 2014; Giessel & Sabatini, 2010; Shinoe, Matsui, Taketo, & Manabe, 2005) further support a major functional role for this receptor subtype in enhancing encoding. However, following M1 activation, the network may become

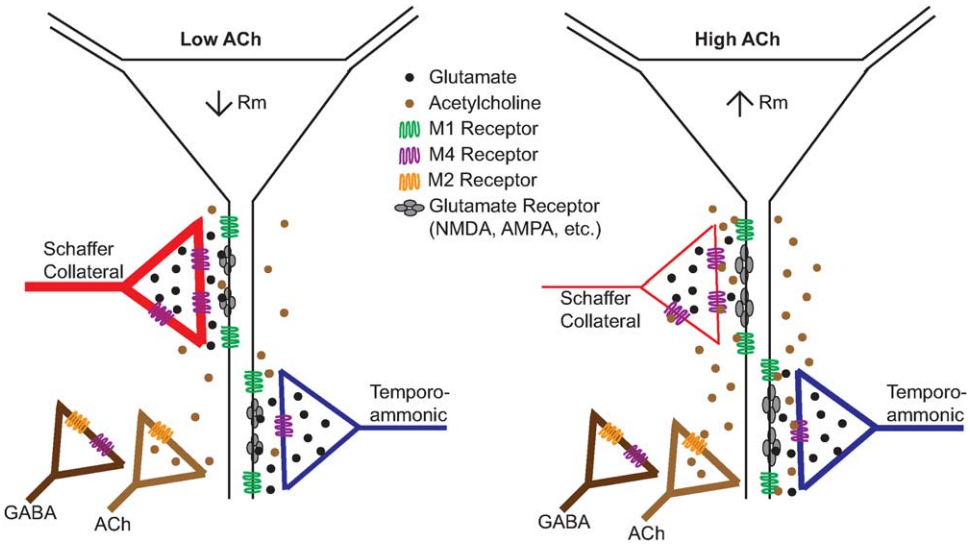


**FIGURE 6** Putative roles of M1 and M4 muscarinic receptors in glutamatergic synaptic transmission in CA1. Left: under conditions of low cholinergic tone, such as occur naturally during sleep, relatively inactivated M4 receptors support heightened release of glutamate, especially from Schaffer collateral synapses. Relatively inactivated M1 receptors reduce the excitability of CA1 pyramidal cells, making them less sensitive to strong glutamatergic inputs. Strong, synchronous activation of SC inputs is thought to support memory retrieval and consolidation functions during resting and sleep. Right: under conditions of high cholinergic tone, which occur naturally during awake exploratory behaviors, activation of M4 receptors leads to a strong presynaptic suppression of SC glutamate release, while TA synaptic transmission remains relatively intact. Activation of postsynaptic M1 receptors makes CA1 pyramidal cells more sensitive to SC and TA glutamatergic inputs. Coordinated activation of SC and TA inputs during this asynchronous state is thought to support plateau potential generation and synaptic plasticity during memory encoding. It is worth noting that mAChRs affect many additional CA1 circuit dynamics, including a prominent role for presynaptic M2 and M4 receptors in modulating transmitter release at septal cholinergic and GABAergic terminals, and GABA release in some interneuron populations (not shown). M1 and M4 also act postsynaptically on a variety of interneuron populations (not shown) to influence circuit dynamics in CA1 [Color figure can be viewed at wileyonlinelibrary.com]

vulnerable to excessive excitation and spurious plasticity. It is noteworthy, therefore, that M1 activation also boosts the intrinsic excitability of fast spiking putative PV+ interneurons, providing one potential mechanism for maintaining balanced excitation and inhibition within CA1 in the intact network. In support of the idea that firing rates in the intact animal may be modulated by such homeostatic mechanisms, one recent study showed that M1 activation failed to increase overall firing in CA1 during memory encoding in awake behaving rats (Lebois et al., 2016). However, the same study did find alterations in synchrony and place field stability within CA1 following the administration of an M1 agonist, consistent with the idea that M1 activation may act to increase intrinsic excitability, cell sensitivity, and synaptic plasticity. By contrast, M4 receptor activation may restrict synaptic modification by reducing excitatory synaptic transmission onto pyramidal cells within CA1 to a sparse population of presynaptic terminals that remain active enough to overcome the SC suppression; these likely include "silent" SC synapses shown to be less affected by muscarinic activation (Buno, Cabezas, & Fernandez de Sevilla, 2006). This reduction of synaptic transmission could potentially also promote the weakening of less active TA inputs via LTD, helping to facilitate appropriate remodeling of the circuitry without excessive excitation. Combined, M1 and M4 activation may thus be sufficient to effectively enhance glutamatergic signal-to-noise ratios within CA1, and to reduce interference of previously learned information during memory encoding—both critical functions of acetylcholine within the hippocampus and other cortical brain regions (Goard & Dan, 2009; Hasselmo & Giocomo, 2006; Kang, Huppe-Gourgues, & Vaucher, 2014; Yu & Dayan, 2002).

Acting through a variety of additional mechanisms, ACh may further promote memory encoding within hippocampal networks. In particular, activation of nicotinic receptors may further spatially and temporally restrict synaptic plasticity by simultaneously enhancing glutamatergic signaling in the SC pathway (Alkondon & Albuquerque, 2002; Lagostena et al., 2010; Nakauchi & Sumikawa, 2012) and enhancing the activity of multiple interneuron populations that inhibit TA synaptic transmission and/or disinhibit pyramidal cells (Bell et al., 2015a; Leao et al., 2012; Nakauchi, Brennan, Boulter, & Sumikawa, 2007).

## 4.3 | Therapeutic activation of M1 and M4 receptors may normalize hippocampal circuit dysfunction in clinical populations

Clarification of the effects of selective M1 and M4 activation has significant clinical relevance, as the cholinergic system has long been one of the most promising therapeutic targets for enhancing learning and memory in dementia disorders. Degeneration of the cholinergic system is observed early in the course of neurodegenerative dementias including Alzheimer's disease, Lewy body dementia, and Parkinson's disease with dementia. The resulting decline in cholinergic tone in the entorhinal-hippocampal network may then result in a CA1 network

state that is unfavorable to the encoding of new memories, and in which Schaffer collateral input to CA1 becomes over-emphasized (Hasselmo & Schnell, 1994), an idea that is supported by recent functional studies in patients with mild cognitive impairment (Bakker et al., 2012; Bakker, Albert, Krauss, Speck, & Gallagher, 2015; Putcha et al., 2011). The results of the present study demonstrate that specific targeting of M1 and M4 receptors may provide improvements in cognitive and behavioral symptoms in these diseases by partially normalizing such aberrant CA1 synaptic activity. Specific targeting of M4 receptors located on presynaptic SC terminals may suppress excessive glutamatergic synaptic activity in the SC pathway, while specific activation of M1 receptors may enhance the sensitivity of CA1 pyramidal neurons and interneurons and facilitate synaptic plasticity. Combined, our results point to mechanisms by which the targeted co-activation of M1 and M4 receptor subtypes could serve to ameliorate the memory deficits suffered by individuals with early stage dementias.

## ACKNOWLEDGMENTS

This work was supported by Pfizer Global Research and Development, Cambridge, MA, USA. The authors thank HDB Biosciences, Rebecca O'Connor, and John Lazzaro for their support of the *in vitro* muscarinic functional assays, and Stephen Jenkinson for his support of the phosphodiesterase and mini-selectivity panels. They also thank Dmitri Volfson for his statistical expertise.

## CONFLICT OF INTEREST

All authors are current or former employees of Pfizer Inc. and own its publicly traded common shares.

## REFERENCES

Abel, T., Havekes, R., Saletin, J. M., & Walker, M. P. (2013). Sleep, plasticity and memory from molecules to whole-brain networks. *Current Biology*, *23*(17), R774–R788.

Alkondon, M., & Albuquerque, E. X. (2002). A non-alpha7 nicotinic acetylcholine receptor modulates excitatory input to hippocampal CA1 interneurons. *Journal of Neurophysiology*, *87*(3), 1651–1654.

Atherton, L. A., Dupret, D., & Mellor, J. R. (2015). Memory trace replay: The shaping of memory consolidation by neuromodulation. *Trends in Neuroscience*, *38*(9), 560–570.

Bakker, A., Albert, M. S., Krauss, G., Speck, C. L., & Gallagher, M. (2015). Response of the medial temporal lobe network in amnestic mild cognitive impairment to therapeutic intervention assessed by fMRI and memory task performance. *Neuroimage: Clinical*, *7*, 688–698.

Bakker, A., Krauss, G. L., Albert, M. S., Speck, C. L., Jones, L. R., Stark, C. E., … Gallagher, M. (2012). Reduction of hippocampal hyperactivity improves cognition in amnestic mild cognitive impairment. *Neuron*, *74*(3), 467–474.

Bates, D., Maechler, M., Bolker, B., & Walker, S. (2015). Fitting linear mixed-effects models using lme4. *Journal of Statistical Software*, *67*(1), 1–48.

Bell, L. A., Bell, K. A., & McQuiston, A. R. (2015a). Acetylcholine release in mouse hippocampal CA1 preferentially activates inhibitory-selective interneurons via alpha4beta2* nicotinic receptor activation. *Frontiers in Cell Neuroscience*, *9*, 115.

Bell, L. A., Bell, K. A., & McQuiston, A. R. (2015b). Activation of muscarinic receptors by ACh release in hippocampal CA1 depolarizes VIP but has varying effects on parvalbumin-expressing basket cells. *Journal of Physiology*, *593*(1), 197–215.

Berridge, M. J. (1993). Inositol trisphosphate and calcium signalling. *Nature*, *361*(6410), 315–325.

Bittner, K. C., Grienberger, C., Vaidya, S. P., Milstein, A. D., Macklin, J. J., Suh, J., … Magee, J. C. (2015). Conjunctive input processing drives feature selectivity in hippocampal CA1 neurons. *Nature Neuroscience*, *18*(8), 1133–1142.

Boddeke, E. W., Enz, A., & Shapiro, G. (1992). SDZ ENS 163, a selective muscarinic M1 receptor agonist, facilitates the induction of long-term potentiation in rat hippocampal slices. *European Journal of Pharmacology*, *222*(1), 21–25.

Bodick, N. C., Offen, W. W., Levey, A. I., Cutler, N. R., Gauthier, S. G., Satlin, A., Shannon, H. E., Tollefson, G. D., Rasmussen, K., Bymaster, F. P., Hurley, D. J., Potter, W. Z., & Paul, S. M. (1997). Effects of xanomeline, a selective muscarinic receptor agonist, on cognitive function and behavioral symptoms in Alzheimer disease. *Archives of Neurology*, *54*(4), 465–473.

Brady, A. E., Jones, C. K., Bridges, T. M., Kennedy, J. P., Thompson, A. D., Heiman, J. U., Breininger, M. L., Gentry, P. R., Yin, H., Jadhav, S. B., Shirey, J. K., Conn, P. J., & Lindsley, C. W. (2008). Centrally active allosteric potentiators of the M4 muscarinic acetylcholine receptor reverse amphetamine-induced hyperlocomotor activity in rats. *Journal of Pharmacology and Experimental Therapeutics*, *327*(3), 941–953.

Brann, M. R., Buckley, N. J., & Bonner, T. I. (1988). The striatum and cerebral cortex express different muscarinic receptor mRNAs. *FEBS Letters*, *230*(1–2), 90–94.

Buchanan, K. A., Petrovic, M. M., Chamberlain, S. E., Marrion, N. V., & Mellor, J. R. (2010). Facilitation of long-term potentiation by muscarinic M(1) receptors is mediated by inhibition of SK channels. *Neuron*, *68*(5), 948–963.

Buckley, N. J., Bonner, T. I., & Brann, M. R. (1988). Localization of a family of muscarinic receptor mRNAs in rat brain. *Journal of Neuroscience*, *8*(12), 4646–4652.

Budzik, B., Garzya, V., Shi, D., Walker, G., Woolley-Roberts, M., Pardoe, J., Lucas, A., Tehan, B., Rivero, R. A., Langmead, C. J., Watson, J., Wu, Z., Forbes, I. T., & Jin, J. (2010). Novel N-substituted benzimidazolones as potent, selective, CNS-penetrant, and orally active M1 mAChR agonists. *ACS Medicinal Chemistry Letters*, *1*(6), 244–248.

Buno, W., Cabezas, C., & Fernandez de Sevilla, D. (2006). Presynaptic muscarinic control of glutamatergic synaptic transmission. *Journal of Molecular Neuroscience*, *30*(1–2), 161–164.

Buzsaki, G. (1989). Two-stage model of memory trace formation: A role for "noisy" brain states. *Neuroscience*, *31*(3), 551–570.

Cea-del Rio, C. A., Lawrence, J. J., Tricoire, L., Erdelyi, F., Szabo, G., & McBain, C. J. (2010). M3 muscarinic acetylcholine receptor expression confers differential cholinergic modulation to neurochemically distinct hippocampal basket cell subtypes. *Journal of Neuroscience*, *30*(17), 6011–6024.

Chan, W. Y., McKinzie, D. L., Bose, S., Mitchell, S. N., Witkin, J. M., Thompson, R. C., Christopoulos, A., Lazareno, S., Birdsall, N. J., Bymaster, F. P., & Felder, C. C. (2008). Allosteric modulation of the muscarinic M4 receptor as an approach to treating schizophrenia. *Proceedings of the National Academy of Sciences of the United States of America*, *105*(31), 10978–10983.

Cutsuridis, V., Cobb, S., & Graham, B. P. (2010). Encoding and retrieval in a model of the hippocampal CA1 microcircuit. *Hippocampus*, *20*(3), 423–446.

Dasari, S., & Gulledge, A. T. (2011). M1 and M4 receptors modulate hippocampal pyramidal neurons. *Journal of Neurophysiology*, *105*(2), 779–792.

Davie, B. J., Christopoulos, A., & Scammells, P. J. (2013). Development of M1 mAChR allosteric and bitopic ligands: Prospective therapeutics for the treatment of cognitive deficits. *ACS Chemistry & Neuroscience*, *4*(7), 1026–1048.

de Vin, F., Choi, S. M., Bolognesi, M. L., & Lefebvre, R. A. (2015). Presynaptic M3 muscarinic cholinoceptors mediate inhibition of excitatory synaptic transmission in area CA1 of rat hippocampus. *Brain Research*, *1629*, 260–269.

Deiana, S., Platt, B., & Riedel, G. (2011). The cholinergic system and spatial learning. *Behavioral Brain Research*, *221*(2), 389–411.

Dennis, S. H., Pasqui, F., Colvin, E. M., Sanger, H., Mogg, A. J., Felder, C. C., Broad, L. M., Fitzjohn, S. M., Isaac, J. T., & Mellor, J. R. (2016). Activation of muscarinic M1 acetylcholine receptors induces long-term potentiation in the hippocampus. *Cerebral Cortex*, *26*(1), 414–426.

Dominguez, S., Fernandez de Sevilla, D., & Buno, W. (2014). Postsynaptic activity reverses the sign of the acetylcholine-induced long-term plasticity of GABAA inhibition. *Proceedings of the National Academy of Sciences of the United States of America*, *111*(26), E2741–E2750.

Drever, B. D., Riedel, G., & Platt, B. (2011). The cholinergic system and hippocampal plasticity. *Behavioral Brain Research*, *221*(2), 505–514.

Dvorak-Carbone, H., & Schuman, E. M. (1999). Long-term depression of temporoammonic-CA1 hippocampal synaptic transmission. *Journal of Neurophysiology*, *81*(3), 1036–1044.

Easton, A., Douchamps, V., Eacott, M., & Lever, C. (2012). A specific role for septohippocampal acetylcholine in memory? *Neuropsychologia*, *50* (13), 3156–3168.

Fernandez de Sevilla, D., & Buno, W. (2003). Presynaptic inhibition of Schaffer collateral synapses by stimulation of hippocampal cholinergic afferent fibres. *European Journal of Neuroscience*, *17*(3), 555–558.

Fisahn, A., Yamada, M., Duttaroy, A., Gan, J. W., Deng, C. X., McBain, C. J., & Wess, J. (2002). Muscarinic induction of hippocampal gamma oscillations requires coupling of the M1 receptor to two mixed cation currents. *Neuron*, *33*(4), 615–624.

Foster, D. J., Choi, D. L., Conn, P. J., & Rook, J. M. (2014). Activation of M1 and M4 muscarinic receptors as potential treatments for Alzheimer's disease and schizophrenia. *Neuropsychiatric Disease and Treatment*, *10*, 183–191.

Gais, S., & Born, J. (2004). Low acetylcholine during slow-wave sleep is critical for declarative memory consolidation. *Proceedings of the National Academy of Sciences of the United States of America*, *101*(7), 2140–2144.

Ghoshal, A., Rook, J. M., Dickerson, J. W., Roop, G. N., Morrison, R. D., Jalan-Sakrikar, N., Lamsal, A., Noetzel, M. J., Poslusney, M. S., Wood, M. R., Melancon, B. J., Stauffer, S. R., Xiang, Z., Daniels, J. S., Niswender, C. M., Jones, C. K., Lindsley, C. W., & Conn, P. J. (2016). Potentiation of M1 muscarinic receptor reverses plasticity deficits and negative and cognitive symptoms in a schizophrenia mouse model. *Neuropsychopharmacology*, *41*(2), 598–610.

Giessel, A. J., & Sabatini, B. L. (2010). M1 muscarinic receptors boost synaptic potentials and calcium influx in dendritic spines by inhibiting postsynaptic SK channels. *Neuron*, *68*(5), 936–947.

Girardeau, G., & Zugaro, M. (2011). Hippocampal ripples and memory consolidation. *Current Opinion in Neurobiology*, *21*(3), 452–459.

Goard, M., & Dan, Y. (2009). Basal forebrain activation enhances cortical coding of natural scenes. *Nature Neuroscience*, *12*(11), 1444–1449.

Hasselmo, M. E. (1999). Neuromodulation: Acetylcholine and memory consolidation. *Trends in Cognitive Science*, *3*(9), 351–359.

Hasselmo, M. E., & Bower, J. M. (1992). Cholinergic suppression specific to intrinsic not afferent fiber synapses in rat piriform (olfactory) cortex. *Journal of Neurophysiology*, *67*(5), 1222–1229.

Hasselmo, M. E., & Giocomo, L. M. (2006). Cholinergic modulation of cortical function. *Journal of Molecular Neuroscience*, *30*(1–2), 133–135.

Hasselmo, M. E., & Schnell, E. (1994). Laminar selectivity of the cholinergic suppression of synaptic transmission in rat hippocampal region CA1: Computational modeling and brain slice physiology. *Journal of Neuroscience*, *14*(6), 3898–3914.

Hasselmo, M. E., Schnell, E., & Barkai, E. (1995). Dynamics of learning and recall at excitatory recurrent synapses and cholinergic modulation in rat hippocampal region CA3. *Journal of Neuroscience*, *15*(7 Pt 2), 5249–5262.

Hasselmo, M. E., & Wyble, B. P. (1997). Free recall and recognition in a network model of the hippocampus: Simulating effects of scopolamine on human memory function. *Behavioral Brain Research*, *89*(1–2), 1–34.

Hersch, S. M., & Levey, A. I. (1995). Diverse pre- and post-synaptic expression of m1-m4 muscarinic receptor proteins in neurons and afferents in the rat neostriatum. *Life Science*, *56*(11–12), 931–938.

Hounsgaard, J. (1978). Presynaptic inhibitory action of acetylcholine in area CA1 of the hippocampus. *Experimental Neurology*, *62*(3), 787–797.

Kaifosh, P., & Losonczy, A. (2016). Mnemonic functions for nonlinear dendritic integration in hippocampal pyramidal circuits. *Neuron*, *90*(3), 622–634.

Kang, J. I., Huppe-Gourgues, F., & Vaucher, E. (2014). Boosting visual cortex function and plasticity with acetylcholine to enhance visual perception. *Frontiers in System Neuroscience*, *8*, 172.

Kenakin, T., Watson, C., Muniz-Medina, V., Christopoulos, A., & Novick, S. (2012). A simple method for quantifying functional selectivity and agonist bias. *ACS Chemistry & Neuroscience*, *3*(3), 193–203.

Kesner, R. P., Kirk, R. A., Yu, Z., Polansky, C., & Musso, N. D. (2016). Dentate gyrus supports slope recognition memory, shades of grey-context pattern separation and recognition memory, and CA3 supports pattern completion for object memory. *Neurobiology of Learning and Memory*, *129*, 29–37.

Kesner, R. P., & Rolls, E. T. (2015). A computational theory of hippocampal function, and tests of the theory: New developments. *Neuroscience & Biobehavioral Reviews*, *48*, 92–147.

Knierim, J. J., & Neunuebel, J. P. (2016). Tracking the flow of hippocampal computation: Pattern separation, pattern completion, and attractor dynamics. *Neurobiology of Learning and Memory*, *129*, 38–49.

Kremin, T., Gerber, D., Giocomo, L. M., Huang, S. Y., Tonegawa, S., & Hasselmo, M. E. (2006). Muscarinic suppression in stratum radiatum of CA1 shows dependence on presynaptic M1 receptors and is not dependent on effects at GABA(B) receptors. *Neurobiology of Learning and Memory*, *85*(2), 153–163.

Kruse, A. C., Kobilka, B. K., Gautam, D., Sexton, P. M., Christopoulos, A., & Wess, J. (2014). Muscarinic acetylcholine receptors: Novel opportunities for drug development. *Nature Reviews Drug Discovery*, *13*(7), 549–560.

Lagostena, L., Danober, L., Challal, S., Lestage, P., Mocaer, E., Trocme-Thibierge, C., & Cherubini, E. (2010). Modulatory effects of S 38232, a non alpha-7 containing nicotine acetylcholine receptor agonist on network activity in the mouse hippocampus. *Neuropharmacology*, *58* (4–5), 806–815.

Leao, R. N., Mikulovic, S., Leao, K. E., Munguba, H., Gezelius, H., Enjin, A., Patra, K., Eriksson, A., Loew, L. M., Tort, A. B., & Kullander, K. (2012). OLM interneurons differentially modulate CA3 and entorhinal inputs to hippocampal CA1 neurons. *Nature Neuroscience*, *15*(11), 1524–1530.

Lenth, R. (2016). Least-squares means: The R package lsmeans. *Journal of Statistical Software*, *69*(1), 1–33.

Leung, L. S., & Peloquin, P. (2010). Cholinergic modulation differs between basal and apical dendritic excitation of hippocampal CA1 pyramidal cells. *Cerebral Cortex*, *20*(8), 1865–1877.

Levey, A. I., Edmunds, S., Koliatsos, M. V., Wiley, R. G., & Heilman, C. J. (1995). Expression of m1-m4 muscarinic acetylcholine receptor proteins in rat hippocampus and regulation by cholinergic innervation. *Journal of Neuroscience*, *15*(5 Pt 2), 4077–4092.

Lindsley, C. W., Conn, P. J., Wood, M. R., Melancon, B. J., Tarr, J. C., & Salovich, J. M. (2013). *Substituted 5-aminothieno[2,3-c]pyridazine-6-carboxamide analogs as positive allosteric modulators of the muscarinic acetylcholine receptor m4*. W. I. P. Organization, Vanderbilt University.

Livermore, D., White, Congreve, K., Brown, M. G., & O'brien, M. (2014). *Piperidin-1-YL and Azipin-1-YL carboxylates as muscarinic M4 receptor agonists*. W. I. P. Organization, Takeda Pharmaceutical Company LTD.

Lu, Z. L., Saldanha, J. W., & Hulme, E. C. (2002). Seven-transmembrane receptors: Crystals clarify. *Trends in Pharmacology Science*, *23*(3), 140–146.

Marr, D. (1971). Simple memory: A theory for archicortex. *Philosophical Transactions of the Royal Society B: Biological Sciences*, *262*(841), 23–81.

Myers, C. E., & Scharfman, H. E. (2011). Pattern separation in the dentate gyrus: A role for the CA3 backprojection. *Hippocampus*, *21*(11), 1190–1215.

Nakauchi, S., Brennan, R. J., Boulter, J., & Sumikawa, K. (2007). Nicotine gates long-term potentiation in the hippocampal CA1 region via the activation of alpha2* nicotinic ACh receptors. *European Journal of Neuroscience*, *25*(9), 2666–2681.

Nakauchi, S., & Sumikawa, K. (2012). Endogenously released ACh and exogenous nicotine differentially facilitate long-term potentiation induction in the hippocampal CA1 region of mice. *European Journal of Neuroscience*, *35*(9), 1381–1395.

Nathan, P. J., Watson, J., Lund, J., Davies, C. H., Peters, G., Dodds, C. M., Swirski, B., Lawrence, P., Bentley, G. D., O'neill, B. V., Robertson, J., Watson, S., Jones, G. A., Maruff, P., Croft, R. J., Laruelle, M., & Bullmore, E. T. (2013). The potent M1 receptor allosteric agonist GSK1034702 improves episodic memory in humans in the nicotine abstinence model of cognitive dysfunction. *International Journal of Neuropsychopharmacology*, *16*(4), 721–731.

Nawaratne, V., Leach, K., Suratman, N., Loiacono, R. E., Felder, C. C., Armbruster, B. N., Roth, B. L., Sexton, P. M., & Christopoulos, A. (2008). New insights into the function of M4 muscarinic acetylcholine receptors gained using a novel allosteric modulator and a DREADD (designer receptor exclusively activated by a designer drug). *Molecular Pharmacology*, *74*(4), 1119–1131.

Neunuebel, J. P., & Knierim, J. J. (2014). CA3 retrieves coherent representations from degraded input: Direct evidence for CA3 pattern completion and dentate gyrus pattern separation. *Neuron*, *81*(2), 416–427.

O'Neill, J., Pleydell-Bouverie, B., Dupret, D., & Csicsvari, J. (2010). Play it again: Reactivation of waking experience and memory. *Trends in Neuroscience*, *33*(5), 220–229.

O'Reilly, R. C., & McClelland, J. L. (1994). Hippocampal conjunctive encoding, storage, and recall: Avoiding a trade-off. *Hippocampus*, *4*(6), 661–682.

Putcha, D., Brickhouse, M., O'keefe, K., Sullivan, C., Rentz, D., Marshall, G., Dickerson, B., & Sperling, R. (2011). Hippocampal hyperactivation associated with cortical thinning in Alzheimer's disease signature regions in non-demented elderly adults. *Journal of Neuroscience*, *31*(48), 17680–17688.

Qian, J., & Saggau, P. (1997). Presynaptic inhibition of synaptic transmission in the rat hippocampus by activation of muscarinic receptors: Involvement of presynaptic calcium influx. *British Journal of Pharmacology*, *122*(3), 511–519.

R Core Team (2016). *R: A language and environment for statistical computing*. Vienna, Austria: R Foundation for Statistical Computing.

Rasmussen, S. G., DeVree, B. T., Zou, Y., Kruse, A. C., Chung, K. Y., Kobilka, T. S., Thian, F. S., Chae, P. S., Pardon, E., Calinski, D., Mathiesen, J. M., Shah, S. T., Lyons, J. A., Caffrey, M., Gellman, S. H., Steyaert, J., Skiniotis, G., Weis, W. I., Sunahara, R. K., & Kobilka, B. K. (2011). Crystal structure of the beta2 adrenergic receptor-Gs protein complex. *Nature*, *477*(7366), 549–555.

Ridler, K., Cunningham, V., Huiban, M., Martarello, L., Pampols-Maso, S., Passchier, J., Gunn, R. N., Searle, G., Abi-Dargham, A., Slifstein, M., Watson, J., Laruelle, M., & Rabiner, E. A. (2014). An evaluation of the brain distribution of [(11)C]GSK1034702, a muscarinic-1 (M 1) positive allosteric modulator in the living human brain using positron emission tomography. *EJNMMI Research*, *4*(1), 66.

Ridley, R. M., Pugh, P., Maclean, C. J., & Baker, H. F. (1999). Severe learning impairment caused by combined immunotoxic lesion of the cholinergic projections to the cortex and hippocampus in monkeys. *Brain Research*, *836*(1–2), 120–138.

Ritz, C., Baty, F., Streibig, J. C., & Gerhard, D. (2015). Dose–response analysis using R. *PLoS One*, *10*(12), e0146021.

Rolls, E. T., & Kesner, R. P. (2006). A computational theory of hippocampal function, and empirical tests of the theory. *Progress in Neurobiology*, *79*(1), 1–48.

Rouse, S. T., Edmunds, S. M., Yi, H., Gilmor, M. L., & Levey, A. I. (2000). Localization of M(2) muscarinic acetylcholine receptor protein in cholinergic and non-cholinergic terminals in rat hippocampus. *Neuroscience Letters*, *284*(3), 182–186.

Sanchez, G., Alvares Lde, O., Oberholzer, M. V., Genro, B., Quillfeldt, J., da Costa, J. C., Cervenansky, C., Jerusalinsky, D., & Kornisiuk, E. (2009). M4 muscarinic receptors are involved in modulation of neurotransmission at synapses of Schaffer collaterals on CA1 hippocampal neurons in rats. *Journal of Neuroscience Research*, *87*(3), 691–700.

Seeger, T., & Alzheimer, C. (2001). Muscarinic activation of inwardly rectifying K(+) conductance reduces EPSPs in rat hippocampal CA1 pyramidal cells. *Journal of Physiology*, *535*(Pt 2), 383–396.

Sheffler, D. J., Williams, R., Bridges, T. M., Xiang, Z., Kane, A. S., Byun, N. E., Jadhav, S., Mock, M. M., Zheng, F., Lewis, L. M., Jones, C. K., Niswender, C. M., Weaver, C. D., Lindsley, C. W., & Conn, P. J. (2009). A novel selective muscarinic acetylcholine receptor subtype 1 antagonist reduces seizures without impairing hippocampus-dependent learning. *Molecular Pharmacology*, *76*(2), 356–368.

Shekhar, A., Potter, W. Z., Lightfoot, J., Lienemann, J., Dube, S., Mallinckrodt, C., Bymaster, F. P., McKinzie, D. L., & Felder, C. C. (2008). Selective muscarinic receptor agonist xanomeline as a novel treatment approach for schizophrenia. *American Journal of Psychiatry*, *165*(8), 1033–1039.

Sheridan, R. D., & Sutor, B. (1990). Presynaptic M1 muscarinic cholinoceptors mediate inhibition of excitatory synaptic transmission in the hippocampus in vitro. *Neuroscience Letters*, *108*(3), 273–278.

Shinoe, T., Matsui, M., Taketo, M. M., & Manabe, T. (2005). Modulation of synaptic plasticity by physiological activation of M1 muscarinic

acetylcholine receptors in the mouse hippocampus. *Journal of Neuroscience*, *25*(48), 11194–11200.

Shirey, J. K., Xiang, Z., Orton, D., Brady, A. E., Johnson, K. A., Williams, R., Ayala, J. E., Rodriguez, A. L., Wess, J., Weaver, D., Niswender, C. M., & Conn, P. J. (2008). An allosteric potentiator of M4 mAChR modulates hippocampal synaptic transmission. *Nature Chemical Biology*, *4*(1), 42–50.

Sutherland, G. R., & McNaughton, B. (2000). Memory trace reactivation in hippocampal and neocortical neuronal ensembles. *Current Opinion in Neurobiology*, *10*(2), 180–186.

Takahashi, H., & Magee, J. C. (2009). Pathway interactions and synaptic plasticity in the dendritic tuft regions of CA1 pyramidal neurons. *Neuron*, *62*(1), 102–111.

Teles-Grilo Ruivo, L. M., & Mellor, J. R. (2013). Cholinergic modulation of hippocampal network function. *Frontiers in Synaptic Neuroscience*, *5*, 2.

Thiele, A. (2013). Muscarinic signaling in the brain. *Annual Review of Neuroscience*, *36*, 271–294.

Treves, A., & Rolls, E. T. (1994). Computational analysis of the role of the hippocampus in memory. *Hippocampus*, *4*(3), 374–391.

Valentino, R. J., & Dingledine, R. (1981). Presynaptic inhibitory effect of acetylcholine in the hippocampus. *Journal of Neuroscience*, *1*(7), 784–792.

Volpicelli, L. A., & Levey, A. I. (2004). Muscarinic acetylcholine receptor subtypes in cerebral cortex and hippocampus. *Progress in Brain Research*, *145*, 59–66.

Weiss, C., Preston, A. R., Oh, M. M., Schwarz, R. D., Welty, D., & Disterhoft, J. F. (2000). The M1 muscarinic agonist CI-1017 facilitates trace eyeblink conditioning in aging rabbits and increases the excitability of CA1 pyramidal neurons. *Journal of Neuroscience*, *20*(2), 783–790.

Wess, J. (1996). Molecular biology of muscarinic acetylcholine receptors. *Critical Reviews in Neurobiology*, *10*(1), 69–99.

Wess, J. (2005). Allosteric binding sites on muscarinic acetylcholine receptors. *Molecular Pharmacology*, *68*(6), 1506–1509.

Wilson, M. A., & Fadel, J. R. (2016). Cholinergic regulation of fear learning and extinction. *Journal of Neuroscience Research*.

Xiang, Z., Thompson, A. D., Jones, C. K., Lindsley, C. W., & Conn, P. J. (2012). Roles of the M1 muscarinic acetylcholine receptor subtype in the regulation of basal ganglia function and implications for the treatment of Parkinson's disease. *Journal of Pharmacology and Experimental Therapeutics*, *340*(3), 595–603.

Yi, F., Ball, J., Stoll, K. E., Satpute, V. C., Mitchell, S. M., Pauli, J. L., Holloway, B. B., Johnston, A. D., Nathanson, N. M., Deisseroth, K., Gerber, D. J., Tonegawa, S., & Lawrence, J. J. (2014). Direct excitation of parvalbumin-positive interneurons by M1 muscarinic acetylcholine receptors: Roles in cellular excitability, inhibitory transmission and cognition. *Journal of Physiology*, *592*(16), 3463–3494.

Yu, A. J., & Dayan, P. (2002). Acetylcholine in cortical inference. *Neural Networks*, *15*(4–6), 719–730.

**How to cite this article:** Thorn C, Popiolek M, Stark E, Edgerton J. Effects of M1 and M4 activation on excitatory synaptic transmission in CA1. *Hippocampus*. 2017;27:794–810. https://doi.org/10.1002/hipo.22732